# ATOMIC FLUORESCENCE SPECTROMETER WITH AN EIMAC CONTINUUM EXCITATION SOURCE AND A GRAPHITE-FILAMENT ATOMIZER

By

FENG-SHYONG CHUANG

A DISSERTATION PRESENTED TO THE GRADUATE COUNCIL OF
THE UNIVERSITY OF FLORIDA IN PARTIAL
FULFILLMENT OF THE REQUIREMENTS FOR THE DEGREE OF
DOCTOR OF PHILOSOPHY

UNIVERSITY OF FLORIDA

1975

# ACKNOWLEDGMENTS

I wish to express my best appreciation to my research advisor, Dr. J. D. Winefordner, for his enthusiastic advice, encouragement, and financial support in the course of this research.

I also wish to express my appreciation to my parents and my wife for their encouragement and sacrifice during the years of my studies.

My gratitude also goes out to my friends, especially Dr. Chuck J. Molnar, for their warm friendship and scholarly assistance ; and also I would like to thank Gail P. Pokrant and T. Ackerman for all their help to me during my studies here.

# TABLE OF CONTENTS

Page

ACKNOWLEDGMENTS . . . . . . . . . . . . . . . . . . . . . . . . . ii

LIST OF TABLES . . . . . . . . . . . . . . . . . . . . . . . . . v

LIST OF FIGURES . . . . . . . . . . . . . . . . . . . . . . . . . vi

ABSTRACT . . . . . . . . . . . . . . . . . . . . . . . . . . viii

Part I

FUNDAMENTAL ASPECTS . . . . . . . . . . . . . . . . . . . . 1

Chapter

I. INTRODUCTION . . . . . . . . . . . . . . . . . . . . . . 1

II. THEORY . . . . . . . . . . . . . . . . . . . . . . . . . 9

Types of Atomic Fluorescence Transitions . . . . . . . 9

Radiance of Atomic Fluorescence Transitions . . . . . 9

Prediction of Atomization Temperature . . . . . . . . . 16

Concentration of Analyte Atoms in Atom Cell . . . . . 17

Interferences . . . . . . . . . . . . . . . . . . . . 21

Time Constants Consideration of Measurement System . . 24

Sheathing Gas Consideration . . . . . . . . . . . . . 25

Noise Consideration . . . . . . . . . . . . . . . . . 26

Limit of Detection . . . . . . . . . . . . . . . . . 26

III. EXPERIMENTAL . . . . . . . . . . . . . . . . . . . . . 28

Reagents . . . . . . . . . . . . . . . . . . . . . . . 28

Experimental System . . . . . . . . . . . . . . . . . 28

Source of Excitation . . . . . . . . . . . . . . . . . 31

Page

Optical System . . . . . . . . . . . . . . . . . . . . . . 31

Electronic Measurement System . . . . . . . . . . . 34

Syringes . . . . . . . . . . . . . . . . . . . . . . . . 34

Atomizer . . . . . . . . . . . . . . . . . . . . . . . . 36

Measurement Procedures . . . . . . . . . . . . . . . 35

Rotameter Calibration . . . . . . . . . . . . . . . . 35

IV. RESULTS AND DISCUSSION . . . . . . . . . . . . . . . 43

Formation of Pyrolytic Carbon on the Graphite-Filament . . . . . . . . . . . . . . . . . . . . . . . . 43

Effect of Ar and $H_2$ Flow Rates upon Atomic Fluorescence Signals . . . . . . . . . . . . . . . . . 43

Influence of Methane Flow Rates on Atomic Fluorescence Signals . . . . . . . . . . . . . . . . . 46

The Influence of Height of Observation upon Fluorescence Signals . . . . . . . . . . . . . . . . . 51

The Influence of Time Constant of Lock-in Amplifier upon Fluorescence Signals and Signal-to-Noise Ratio . . . . . . . . . . . . . . . . 51

Analytical Figures of Merit . . . . . . . . . . . . . 60

Precision . . . . . . . . . . . . . . . . . . . . . . . 62

Part II

APPLICATIONS . . . . . . . . . . . . . . . . . . . . . 67

Introduction . . . . . . . . . . . . . . . . . . . . . 67

Experimental . . . . . . . . . . . . . . . . . . . . . 68

Results and Discussion . . . . . . . . . . . . . . . . 68

REFERENCES . . . . . . . . . . . . . . . . . . . . . . . 73

BIOGRAPHICAL SKETCH . . . . . . . . . . . . . . . . . . 77

# LIST OF TABLES

Table Page

1 Some Major Types of Non-Flame Atomizers . . . . . . 7

2 Thermodynamic Reduction Temperatures and Appearance Temperatures for 27 Elements Undergoing Carbon-Furnace Atomization . . . . . . . . . . . . . . . . . 18

3 Experimental Conditions for Atomic Fluorescence Spectrometer with EIMAC Xenon Arc Lamp and Graphite-Filament Atomizer . . . . . . . . . . . . 38

4 The Influence of Hydrogen Gas Upon Fluorescence and Absorption Signals . . . . . . . . . . . . . . . 47

5 Limits of Detection Measured for Several Elements in Present Work and in Other Studies . . . . . . . 63

6 Comparison of Silver and Copper Determination in Jet Engine Oils . . . . . . . . . . . . . . . . . 72

## LIST OF FIGURES

Figure Page

1. Basic instrumental system for atomic emission (AE), atomic absorption (AA), and atomic fluorescence (AF), spectrometry . . . . . . . . . . . . . . . . . . . . 2

2. Types of atomic fluorescence transitions . . . . . . . . . 10

3. Atomic fluorescence growth curve with a line source of excitation . . . . . . . . . . . . . . . . . . . . . . . . 14

4. Atomic fluorescence growth curve with a continuum source of excitation . . . . . . . . . . . . . . . . . . . . . . . 15

5. Schematic diagram of an atomic fluorescence spectrometer with an EIMAC continuum source and graphite-filament atomizer . . . . . . . . . . . . . . . . . . . . . . . . . 29

6. Spectral characteristics of the EIMAC xenon arc continuum lamp used in this study . . . . . . . . . . . . 32

7. Time-stability of the EIMAC xenon arc lamp used in this study . . . . . . . . . . . . . . . . . . . . . . . . 33

8. Schematic diagram of graphite-filament atomizer . . . . . 36

9. Argon flow rate versus rotameter reading at 85 pounds pressure . . . . . . . . . . . . . . . . . . . . . . . 40

10. Hydrogen flow rate versus rotameter reading at 8 pounds pressure . . . . . . . . . . . . . . . . . . . . . . 41

11. Methane flow rate versus rotameter reading at 10 pounds pressure . . . . . . . . . . . . . . . . . . . . . 42

12. Influence of argon flow rates on fluorescence signals of various elements . . . . . . . . . . . . . . . . 45

13. Influence of hydrogen flow rates on fluorescence signals of various elements . . . . . . . . . . . . . . . . 49

14. Influence of methane flow rates on fluorescence signals of various elements . . . . . . . . . . . . . . . . 50

Figure Page

15. Influence of height of observation upon silver fluorescence signals . . . . . . . . . . . . . . 52

16. Influence of height of observation upon cadmium fluorescence signals . . . . . . . . . . . . . . 53

17. Influence of height of observation upon chromium fluorescence signals . . . . . . . . . . . . . . 54

18. Influence of height of observation upon copper fluorescence signals . . . . . . . . . . . . . . 55

19. Influence of height of observation upon iron fluorescence signals . . . . . . . . . . . . . . 56

20. Influence of height of observation upon magnesium fluorescence signals . . . . . . . . . . . . . . 57

21. Influence of height of observation upon lead fluorescence signals . . . . . . . . . . . . . . 58

22. Influence of height of observation upon tin fluorescence signals . . . . . . . . . . . . . . 59

23. Atomic fluorescence calibration curves for thirteen elements . . . . . . . . . . . . . . . . . 61

24. Examples of temporal characteristic of atomic fluorescence signals resulting from sequential atomization of silver and copper . . . . . . . . 70

25. Atomic fluorescence analytical calibration curves for sequential determination of silver and copper 71

Abstract of Dissertation Presented to the Graduate Council
of the University of Florida in Partial Fulfillment of the
Requirements for the Degree of Doctor of Philosophy

# ATOMIC FLUORESCENCE SPECTROMETER WITH AN EIMAC CONTINUUM EXCITATION SOURCE AND A GRAPHITE-FILAMENT ATOMIZER

By

Feng-Shyong Chuang

June, 1975

Chairman: James D. Winefordner
Major Department: Chemistry

A graphite-filament atomizer is used to produce atoms for a variety of elements, and the resulting atomic vapor is excited by means of an EIMAC xenon arc continuum source. The resulting atomic fluorescence is measured by a conventional atomic fluorescence spectrometric instrumental system. Detection limits (sample size of 0.5 - 1.0 μl) are in the range of $2 \times 10^{-4}$ to 0.1 μg/ml and 0.2 - 50 pg for Ag, Cd, Co, Cu, Cr, Fe, Mg, Mn, Ni, Pb, Sn, Tl, and Zn. Relative standard deviations (for four measurements) ranged from 0.03 to 0.07 for all of the above. The atomic fluorescence spectrometric system is simple and inexpensive to construct, simple to operate, and useful for a variety of elements without the need of changing any instrumental component or parameter other than the wavelength of the monochromator and possibly the conditions of atomization.

The application of the sequential determination of silver and copper in jet engine oils with this system is also studied. The analytical results are quite satisfactory compared with the mean value of U.S. Air Force SOAP laboratory obtained by atomic absorption flame spectrometry.

# PART I - FUNDAMENTAL ASPECTS

## CHAPTER I

## INTRODUCTION

Trace element analysis is becoming increasingly important in medicine, geology, food, and pollution. Dependable, sensitive, precise, and simple methods of analysis are required to satisfy the needs of a worker in these areas. The three commonly used atomic spectroscopic methods for trace metal analysis are based upon atomic emission (AES), atomic absorption (AAS), and atomic fluorescence (AFS) spectrometry.

Atomic emission, atomic absorption and atomic fluorescence spectrometry differ in the mechanism of excitation and the means of measurement of characteristic signals. In atomic emission, the analyte atoms are excited via collisional means with a flame gas molecule, and a portion of the radiation emitted when a fraction of the excited atoms undergoes radiational deactivation is measured. In atomic absorption, the analyte atoms are excited by means of an external light source, and the fraction radiation absorbed from the light source as a result of radiational excitation is measured. In atomic fluorescence, the analyte atoms are again excited as in atomic absorption, but a portion of the atomic fluorescence radiation resulting when a fraction of the excited atoms undergo radiational deactivation is measured. The basic excitation mechanism and instrumental systems for these methods are shown in Figure 1.

In all flame spectrometric methods, sample solutions (containing the analyte) are nebulized and introduced into a flame as an aerosol.

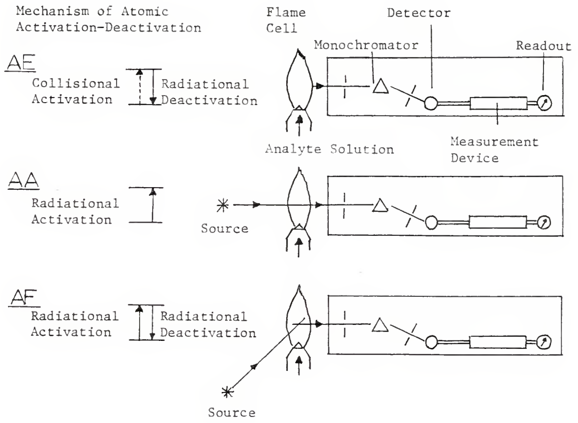

Fig. 1. Basic instrumental system for atomic emission (AE), atomic absorption (AA), and atomic fluorescence (AF) spectrometry.

Within the flame, the solvent evaporates from the resulting aerosol to produce solute particles which then vaporize to produce atoms, ions, and molecules. The production of analyte atoms in the flame are essential to the measurements of atomic emission, atomic absorption, and atomic fluorescence.

The historical development and detailed experimental arrangement of (flame) atomic emission and atomic absorption are not described here because the present work is primarily concerned with atomic fluorescence. However, the author will discuss, in a rather detailed manner, atomic fluorescence including historical, theoretical, and experimental developments and results.

Wood (1) observed atomic fluorescence of sodium vapor in 1905. Nichols and Howes (2) reported the atomic fluorescence of Ba, Ca, Li, Na, and Sr in a flame in 1924, and 1929. Badger (3) published a paper on atomic fluorescence of Ag, Cd, Cu, Hg, Na, and Tl. The most significant paper leading to the analytical development of flame atomic fluorescence (FAFS) was by Alkemade (4). Winefordner (5) published the first paper in 1964 on flame atomic fluorescence spectrometry for analytical use. T.S. West (6) also reported the uses of atomic fluorescence in analytical chemistry in 1966.

Because the fluorescence intensity is linearly proportional to the intensity of light source, one of the major research areas in atomic fluorescence spectrometry has been the development of a suitable light source. The most commonly used sources of excitation include cw (continuum wave) electrodeless discharge lamps (EDL) operated at microwave frequencies with an "A"-antenna or a cavity for coupling the microwaves to the EDL; pulsed hollow cathode discharge lamps; xenon arc continuum sources; and cw and pulsed tunable dye lasers. Thermostatted single element and multielement EDLs (7-9) have been shown to give higher stabilities, higher intensities, and longer lifetimes than non-thermostatted EDLs. Tunable dye lasers have very high intensities and very high potential for use; however, they are expensive and unable to excite spectral lines with wavelengths shorter than ≈260 nm.

In atomic fluorescence spectrometry, the source radiation is chopped resulting in a modulated fluorescence signal, which can be electronically separated from the constant background cell emission signals by means of a tuned AC amplifier, such as a phase-sensitive lock-in amplifier.

Types of flames used in atomic fluorescence spectrometry are similiar to those used in flame atomic absorption spectrometry. Air-acetylene and nitrous oxide-acetylene flames are predominately used at the present time. However, the use of the flame as an atomizer has some disadvantages. First, the flicker of the flame causes a considerable flame flicker noise which results in a decreased signal-to-noise ratio. Second, the flame contains quenching species, such as $N_2$, CO, $CO_2$, and $H_2O$, etc., which quench the excited species and result in a reduction of the fluorescence signal. Third, a very small amount of sample (in μl range), which is often required in both clinical and air-borne particle measurements, is difficult to analyze by flame atomic fluorescence spectrometry. However, the use of a non-flame atomizer overcomes many of the limitations resulting from a flame atomizer. Non-flame atomizers generally result in lower absolute and often concentrational detection limits than conventional flames, whether atomic absorption or fluorescence measurement is utilized. Also, such devices provide a reducing and inert atmosphere around the graphite rod and also provide a relatively high atomization temperature (up to 3000 °C).

L'vov has been a pioneer in the field of resistively heated non-flame cell atomic absorption spectroscopy; he has developed a graphite tube furnace contained in an inert atmosphere for intensive atomic absorption studies (10-15). A complete review of his work is included in his text (16). Massmann also developed a resistively heated graphite cuvette atomization cell suitable for both atomic absorption and atomic fluorescence spectrometries (17-18). Woodriff (19-22) determined mercury in air samples via atomic absorption spectrometry with both a carbon cup (23) and a carbon rod (24). The L'vov type, Woodriff type, Massmann type, and Varian type of carbon furnace atomizers for atomic absorption spectrometry have been reviewed by Woodriff (25), concerning their advantages, disadvantages, and the effects of sample introduction system in relation to accuracy, sensitivity, and convenience.

The tube furnace atomizers generally result in greater absorption sensitivities, achieve lower limits of detection, and are less prone to interferences than filament type of atomizers. However, because of the complexity of the tube furnace design, more power is required and more time is needed for analytical measurement, and so more emphasis for routine application has been placed on the simpler graphite-filament (GFA) and graphite-rod (GRA) atomizers. West and co-workers (26-33) developed the graphite-filament atomizer and studied its applicability to a wide range of metals, using both atomic absorption and atomic fluorescence spectroscopy. They found that, in general, there was no change in sensitivity for copper, silver, zinc, cadminum, iron, and lead with changes in complexing agents or salts and for metal complexes extracted into organic solvents. A number of cations were found to interfere, but the extent of interference could be reduced by restricting the position of measurement to the area immediately above the graphite rod. West et al. later used the same system with a little modification to analyze phosphorus and sulfur in aqueous solution (34), and developed a carbon-tube atomizer for the determination of iodine by atomic absorption spectrometry (35). Matoušek and co-workers (36) designed a carbon rod atomizer for atomic absorption and atomic fluorescence spectrometry. The same carbon rod atomizer was used to analyze the trace amount of magnesium, iron, copper, lead, and zinc in blood and plasma (37) and directly determine silver, aluminum, copper, chromium, magnesium, nickel, and lead in lubricant oils (38). Winefordner's group has used the graphite-filament (39) to measure wear metals (Ag, Cu, Cr, Fe, Mg, Ni, Pb, and Sn) in jet engine oils (40-42), trace elements (Mg, Fe and Cu) in blood serum (41, 43, 44) by atomic absorption; and to analyze copper and silver sequentially and simultaneously in oils by both atomic absorption (45) and atomic fluorescence (46) spectrometry. The metal filament loop system is used primarily for more volatile elements. Winefordner et al. have also employed a resistively heated Pt filament as an atomizer for atomic fluorescence spectrometry (47). Hwang (48,49) used a tantalum strip and a tantalum ribbon in an enclosed inert atmosphere to analyze lead in blood serum; and to determine thirty-seven elements by atomic absorption spectrometry respectively. Continuously fed sample into a graphite furnace was utilized by Molnar and Winefordner (50) for atomic fluorescence measurements and by Veillon (51,52) for both atomic absorption and atomic fluorescence spectroscopy. Several major types of non-flame atomizers are listed in Table 1. However, there are various types of non-flame atomizers which will not be mentioned here. The interested

TABLE 1

SOME MAJOR TYPES OF NON-FLAME ATOMIZER

Graphite Filament (or Rod) Types:

| Author | Means of Measurement | References |
|---|---|---|
| T.S. West | AA, AF | (26-33) |
| J.P. Matoušek | AA | (36-38) |
| J.D. Winefordner | AA, AF | (39-46) |

Graphite Tube Furnace Types:

| Author | Means of Measurement | References |
|---|---|---|
| B.V. L'vov | AA | (10-16) |
| R. Woodriff | AA | (19-22),(56) |
| H. Massmann | AA, AF | (17-18) |
| Instrumental Lab. | AA | (57) |
| Perkin-Elmer | AA | (59) |
| J.D. Winefordner | AF | (50) |
| C. Veillon | AA, AF | (51-52) |

Metallic Loop (or Strip) Types:

| Author | Means of Measurement | References |
|---|---|---|
| J.D. Winefordner (Pt loop) | AF | (47) |
| J.Y. Hwang (Ta strip) | AA | (48-49) |
| E.H. Piepmeimer (W filament) | AA | (58) |

AA: Atomic Absorption Method

AF: Atomic Fluorescence Method

reader may refer to the excellent reviews of non-flame atomizers by Kirkbright (53), and Winefordner and Vickers (54,55) who have given thorough discussions on many of them.

The purpose of this thesis project was to develop an economic, convenient, versatile, sensitive, and precise graphite-filament atomic fluorescence spectrometry with an EIMAC xenon arc continuum source. The analytical figures of merit for thirteen elements, a method of producing pyrolytic carbon on the filament to the atomic fluorescence spectrometry, the influence of shield gas flow rates ($H_2$, Ar, and $CH_4$) on fluorescence intensity, and the factors affecting measurements of precision and detection limits are studied. The application of using this system for the rapid sequential analysis of Ag and Cu in jet engine oils is also reported.

# CHAPTER II

# THEORY

## Types of Atomic Fluorescence Transitions

The types of atomic fluorescence transitions are (1) Resonance Fluorescence, in which the same lower and upper levels are involved in the excitation-deexcitation processes. (2) Direct Line Fluorescence, in which the same upper level is involved in the radiational excitation and deexcitation processes. (3) Step-Line Fluorescence, in which different upper levels are involved in the radiational excitation and deexcitation processes. If the fluorescence energy is greater than the excitation energy, then this type of fluorescence is called an Anti-Stokes process; and if the reverse is true, the type of fluorescence is then termed a Stokes process. A few types of atomic fluorescence transitions are shown in Figure 2. For a more detailed discussion about the types of fluorescence transitions, refer to the article by Omenetto and Winefordner (60).

## Radiance of Atomic Fluorescence Transitions

Winefordner et al.(5,61,62) have theoretically derived and experimentally verified expressions to describe the relationships between the fluorescence intensity and the number of ground state atoms for several limiting but experimentally useful cases with the following assumptions:

(i) The sample cell is completely illuminated, and the fluorescence emanating at right angles to the exciting beam from the cell

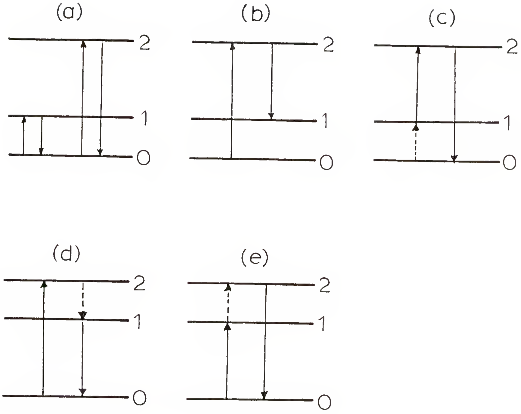

Fig. 2. Types of atomic fluorescence transitions.
(a) Resonance fluorescence.
(b) Stokes direct line fluorescence.
(c) Anti-Stokes direct line fluorescence.
(d) Stokes stepwise line fluorescence.
(e) Anti-Stokes stepwise line fluorescence.

The solid lines represent radiational processes, and the dashed lines represent non-radiational processes.

toward the detector is measured.

(ii) Both the exciting radiation reaching the cell and the measured fluorescence radiation are collimated beams, but perpendicular to each other.

(iii) If a continuum source is used, the continuum source must have a constant spectral radiance over the absorption line width; and if a line source is used, the line source must have a small half-width compared to the absorption line half-width.

(iv) The atomic concentration and the temperature of the atomizer at the height of measurement are constant across the atomizer.

If a line source is used to excite low concentration analyte atoms ($n_0$), the following equation holds for the atomic fluorescence radiance $B_F$(erg $s^{-1}$ $cm^{-2}$ $sr^{-1}$)

$$B_F = K_{1u}\, n_0\, X_1\, f_{1u}\, \delta_{1u}\, B_s\, Y' \left(\frac{\Omega}{4\pi}\right)\left(\frac{Ll1'}{A_s}\right) \qquad \text{II-1}$$

where

$K_{1u}$ = modified atomic absorption coefficient for pure Doppler broadening ($cm^2 sr^{-1}$),

$n_0$ = concentration of the atoms in the ground state ($cm^{-3}$),

$X_1$ = fraction of analyte atom in the lower state involved in the absorption transition (dimensionless),

$f_{1u}$ = absorption oscillator strength for transition 1→u, where 1 is the lower state and u is the upper state (dimensionless),

$\delta_{1u}$ = factor to account for finite half-width of the line source compared to the absorption line (dimensionless),

$B_s$ = radiance of line source (erg $s^{-1}$ $cm^{-2}$ $sr^{-1}$),

Y' = fluorescence power yield (dimensionless),

$\Omega$ = solid angle of exciting radiation collected from source and impinging upon the flame (sr),

$L, l, l'$ = absorption path length, fluorescence path length, and measurement height (cm),

$A_s$ = total atomizer cell surface ($cm^2$).

At high analyte concentration (high $n_0$), the atomic fluorescence radiance $B_F$ with line excitation source is

$$B_F = 2B_s\, l'\, Y'\, \left(\frac{\Omega}{4\pi}\right) \sqrt{\frac{a_F\, L}{\sqrt{\pi}\, K_F\, n_0\, X_F\, f_F}}\, \left(\frac{1}{A_s}\right) \qquad \text{II-2}$$

where

$a_F$ = damping constant for atomic fluorescence (dimensionless),

$K_F$ = modified absorption coefficient (same as $K_{lu}$) but for reabsorption of fluorescence ($cm^2\ sr^{-1}$),

$X_F$ = fraction of atoms in lower state involved in reabsorption of fluorescence (dimensionless),

$f_F$ = absorption oscillator strength for reabsorption of fluorescence (dimensionless).

If a continuum excitation source is used, the relationship between the fluorescence radiance $B_F$ and low concentration analyte atoms ($n_0$) is

$$B_F = C_1\, K_{lu}\, n_0\, X_1\, f_{lu}\, \Delta\lambda_D\, B_{c\lambda_{lu}}\, Y'\, \left(\frac{\Omega}{4\pi}\right) \sqrt{\frac{C_2\, l\, L}{\sqrt{\pi}}}\, \left(\frac{1}{A_s}\right) \qquad \text{II-3}$$

where

$C_1$ = $\frac{\sqrt{\pi}}{2(\ln 2)^{\frac{1}{2}}}$ (dimensionless),

$\Delta\lambda_D$ = Doppler half-width of the absorption line (nm),

$\lambda_{lu}$ = absorption line peak for transition $l \rightarrow u$ (cm),

$B_{c\lambda_{lu}}$ = spectral radiance for continuum source (erg $s^{-1}\ cm^{-2}\ sr^{-1}\ nm^{-1}$).

At high optical density (high $n_0$), the atomic fluorescence radiance with a continuum source is equal to

$$B_F = 2B_{c\lambda_{1u}} \Delta\lambda_D \, a_F \, l' \, Y' \left(\frac{\Omega}{4\pi}\right) \sqrt{\frac{C_2 \, l \, L}{\sqrt{\pi}}} \left(\frac{1}{A_s}\right) \qquad \text{II-4}$$

where

$$C_2 = \frac{\sqrt{\pi}}{\ln 2}$$

According to equations II-1 to II-4, the following analytically-useful conclusions can be made:

(i) the fluorescence radiance depends directly on the intensity of the source radiation, the fluorescence yield (Y'), and the excited and collected solid angles;

(ii) If the atomic concentration ($n_0$) is low, the fluorescence radiance is linearly related to $n_0$, whatever the source of excitation and whatever the cell shape. However, at high $n_0$ values, the fluorescence radiance is independent of $n_0$ when a continuum excitation source is used, and is dependent on $\sqrt{\frac{1}{n_0}}$ when a line excitation source is used. Therefore, atomic fluorescence spectrometry is primarily useful for the measurement of low analyte concentration or trace analysis;

(iii) the analytical curve, obtained by plotting log S, ie., s = signal, (or log $B_F$) vs log C (or log $n_0$), has a slope equal to unity at low $n_0$, whatever the source of excitation used. The slope is equal to zero at high $n_0$ when continuum excitation source is used, and equal to $\frac{-1}{2}$ at high $n_0$ when line excitation source is used.

Typical analytical curves are shown in Figures 3 and 4.

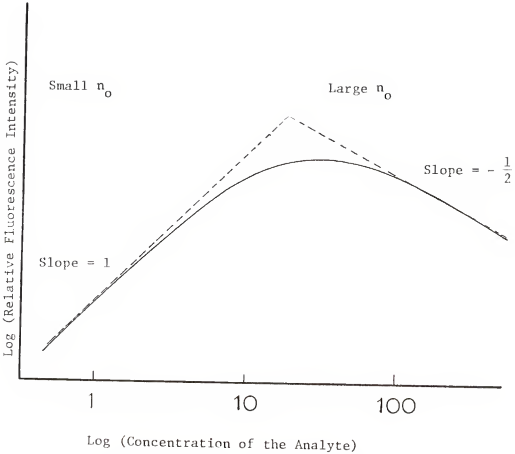

Fig. 3. Atomic fluorescence growth curve with a line source of excitation.

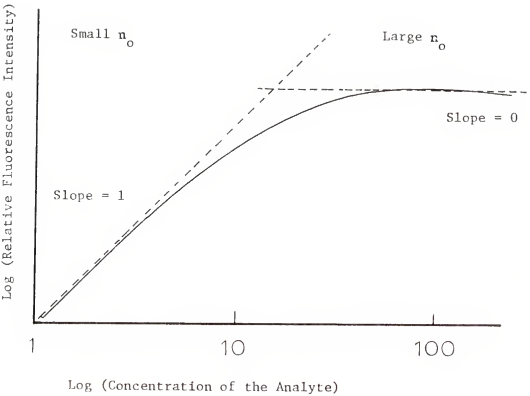

Fig. 4. Atomic fluorescence growth curve with a continuum source of excitation.

## Prediction of Atomization Temperatures

Because of the difference of atomization behavior of the analyte with a graphite furnace atomizer compared with a flame atomizer, the atomization temperature of the analyte will be different with these two types of atomizers,e.g., the flame atomizer contains radicals, such as O and OH, which form stable compounds with the analyte; however, the graphite furnace contains primarily inert gas molecules.

If a particle containing $MgSO_4$ is heated, $MgSO_4(s)$ will form $MgO(s)$ at 890°C which will sublime without decomposition at 2770°C. However, very sensitive determinations of Mg can be obtained at temperatures as low as 1550°C. This (and other) evidence leads to the conclusion that carbon plays a role in atom production (63).

Metal solutions of oxy-anion salts (sulfates and nitrates) and metallo-organic compound (Conostan and SOAP standards) decomposed to the corresponding metal oxide in heating. A possible model for the formation of metal atoms would therefore be the reduction of the metal oxide by carbon as the following equation shows (63).

$$MO(s) + C(s) \longrightarrow CO(g) + M(g) \qquad \text{II-5}$$

where M is the atom being atomized. This model assumes that sufficient energy is released on the formation of carbon monoxide to produce metal atoms directly in the gaseous state rather than in intermediate solid or liquid states. If it is assumed that the above reaction equation occurs in thermodynamic equilibrium near the surface of the graphite atomizer, then it is possible to use free-energy data to calculate the overall free-energy change of the reaction. The overall free-energy change will vary with temperature but will become negative at some temperature above which the reaction is thermodynamically feasible. This temperature should be related to the lowest temperature at which a substantial population of atoms is observed in the graphite atomizer. This approach takes no account of reaction rates, but it is generally assumed that at high temperatures, reaction rates for carbon reduction of oxides are rapid if the reaction has a negative free-energy change.

Example: To predict the atomization temperature of $Al_2(SO_4)_3$ in a graphite furnance atomizer:

$$2\ Al_2(SO_4)_3(s) \longrightarrow 2\ Al_2O_3(s) + 6\ SO_2 + 3\ O_2$$

$$Al_2O_3(s) + 3\ C(s) \longrightarrow 3\ CO(g) + 2\ Al(g)$$

The overall free-energy change, $\Delta G^o$, for this reaction will be given by the sum of the free energies of formation of the reaction, ie.,

$$\Delta G^o_{reaction} = 2\ \Delta G^o_f Al(g) + 3\ \Delta G^o_f CO(g) - \Delta G^o_f Al_2O_3(s) - 3\ \Delta G^o_f C(s)$$

at 2400°K

$$\Delta G^o_{reaction} = (2 \times 8.72 \text{ Kcal/mole}) + 3\text{x}(-76.28 \text{ Kcal/mol}) - (-218.36 \text{ Kcal/mol}) - (0 \text{ Kcal/mol}) = 6.97 \text{ Kcal/mol}$$

at 2500°K

$$\Delta G^o_{reaction} = (2 \times 6.12 \text{ Kcal/mol}) + 3\text{x}(-78.25 \text{ Kcal/mol}) - (-212.09 \text{ Kcal/mol}) - (0 \text{ Kcal/mol}) = -10.42 \text{ Kcal/mol}.$$

Therefore, the values predict that the release of aluminium atoms becomes thermodynamically feasible between 2400°K and 2500°K. The thermodynamic reduction temperatures and experimental appearance temperatures for 27 elements are shown in Table 2.

## Concentration of Analyte Atoms in Atom Cell

The concentration of analyte atoms in flame (atoms $cm^{-3}$) is related to the concentration of analyte (mol $l^{-1}$) in the solution aspirated into the flame (5,64,65) by

## TABLE 2

## THERMODYNAMIC REDUCTION TEMPERATURES AND APPEARANCE TEMPERATURES FOR 27 ELEMENTS UNDERGOING CARBON FURNACE ATOMIZATION (63)

(The melting and boiling points of the elements are included for comparison.)

| Oxide | Element m.p. °K | Element b.p. °K | Temperature °K at which $\Delta G^o$ reaction is negative | Appearance temperature of element °K |
|---|---|---|---|---|
| PbO | 600 | 2024 | 1000-1100 | 1000 |
| $Al_2O_3$ | 932 | 2720 | 2400-2500 | 2300 |
| $Cu_2O$ | 1366 | 2855 | 1800-1900 | 1730 |
| $Fe_3O_4$ | 1812 | 3160 | 1700-1800 | 1750 |
| $Na_2O$ | 371 | 1163 | 1200-1300 | 1230 |
| NiO | 1728 | 3110 | 1700-1800 | 1800 |
| $Cr_2O_3$ | 2176 | 2915 | 1800-1900 | 1800 |
| ZnO | 693 | 1181 | 1200 | 1100 |
| CoO | 1768 | 3150 | 1800 | 1720 |
| $Sc_2O_3$ | 1673 | 2750 | 2400-2500 | 2450 |
| CdO | 594 | 1038 | >800 | 850 |
| $V_2O_3$ | 2190 | 3650 | 2400-2500 | 2350 |
| $SiO_2$ | 1683 | 2950 | 2300 | 2300 |
| BaO | 983 | 1910 | 2300 | 2200 |
| $TiO_2$ | 1950 | 3550 | 2400-2500 | 2420 |
| $LiO_2$ | 454 | 1604 | 1900-2000 | 2100 |
| $Mn_3O_4$ | 1517 | 2314 | 1600-1700 | 1600 |
| $Ag_2O$ | 1234 | 2450 | 1200-1300 | 1150 |
| SrO | 1043 | 1640 | 2300 | 2100 |
| HgO | 234 | 629 | Below room temperature | — |
| $B_2O_3$ | 2300 | 4200 | $\Delta G^o$ reaction is + at b.p. | — |
| NbO | 2770 | 5200 | 3000 | — |
| $SnO_2$ | 505 | 2960 | 1350 | 1800 |

Table 2 - continued

| Oxide | Element m.p. °K | Element b.p. °K | Temperature °K at which $\Delta G^o$ reaction is negative | Appearance temperature of element °K |
|---|---|---|---|---|
| $K_2O$ | 336 | 1039 | 1100 | 1550 |
| $Sb_2O_3$ | 903 | 1910 | 1100-1200 | 1550 |
| CaO | 1123 | 1765 | 2400-2500 | 1800 |
| MgO | 923 | 1390 | 2100-2200 | 1550 |

$$n_f = 1 \times 10^9 \frac{F \varepsilon \beta C}{Q e_f} \qquad \text{II-6}$$

where

$n_f$ = total concentration of atoms when flame is used as atomizer ($cm^3$),

F = solution transport rate ($cm^3\ min^{-1}$),

$\varepsilon$ = efficiency of aspiration, ie., efficiency of producing gaseous analyte in the flame (dimensionless)

$\beta$ = efficiency of atomization, ie., efficiency of producing atoms from gaseous analyte (dimensionless),

$e_f$ = flame gas expansion factor due to increase in temperature of gas from room temperature and increase in number of moles of flame gas products (dimensionless)

Q = flow rate of unburnt gases into flame ($cm^3\ s^{-1}$).

The atomization efficiency, $\beta$ , is the ratio of the concentration of free analyte atoms in the flame to the total concentration of analyte in all gaseous forms. This factor corrects for incomplete dissociation of the analyte compound, combination of analyte atoms with flame gas molecules, and ionization of analyte atoms in the flame. The aspiration efficiency, $\varepsilon$ , is the ratio of the number of all gaseous analyte species produced in the flame per unit time to the number of analyte species aspirated per unit time. This factor corrects for the loss of analyte solution in the nebulizer and associated tubing and the incomplete volatization of the solid particles in the flame gases.

The atomic concentration (atom $cm^{-3}$) produced from a graphite-filament atomizer cavity is related to the concentration of analyte (65) by

$$n_g = 6 \times 10^{20} \, V \, C \, \varepsilon \beta / V_g \qquad \text{II-7}$$

if the analyte vaporizes instantly, diffuses slowly; and the system is in static state.

Where

$n_g$ = total concentration of atoms when graphite-filament as atomizer ($cm^{-3}$),

$V$ = volume of analyte solution introduced into the cell ($cm^3$),

$V_g$ = volume of the graphite-filament cavity ($cm^3$).

Dividing equation II-6 by II-7, the ratio of atomic concentration assuming the same concentration of analyte is introduced either into the flame or graphite-filament is given by the equation (66)

$$R_n = 60 \left(\frac{V}{V_g}\right) (\varepsilon\beta)_g / \left(\frac{F}{Qe_f}\right) (\varepsilon\beta)_f \qquad \text{II-8}$$

where

$(\varepsilon\beta)_g$ = $\varepsilon\beta$ value of analyte atomized via graphite-filament atomizer,

$(\varepsilon\beta)_f$ = $\varepsilon\beta$ value of analyte atomized via flame atomizer.

To compare the gain ($R_n$) of atom production between the graphite-filament atomizer and flame atomizer, several parametreal values are chosen: $V = 0.0005\ cm^3$, $V_g = 0.002\ cm^3$, $(\varepsilon\beta)_g = 1$, $(\varepsilon\beta)_f = 1$, $F = 2\ cm^3 min^{-1}$, $Q = 100\ cm^3\ s^{-1}$, $e_f = 10$. For this particular case, $R_n = 7500$, which shows that the graphite-filament atomizer should generate a much greater atomic concentration than the flame cell.

## Interferences

The three major types of interferences which occur in all types of atomic spectrometry are classified as spectral interference, chemical interference, and physical interference. Spectral interference can occur only when there is spectral overlap between the analyte resonance line and the interferent line or band. In atomic absorption and atomic fluorescence with modulated line sources and tuned detector, spectral interferences are not nearly as important because the absorption (and fluorescence) lines are so narrow (about 0.1 A). However, atomic emission, atomic absorption with a continuum excitation source, and atomic fluorescence with a continuum excitation source will suffer spectral interferences if any interferent has spectral lines or bands within the spectral bandwidth of the monochromator. Spectral interferences can be reduced by decreasing the spectral bandwidth of the monochromator.

Chemical interferences are usually the result of incomplete dissociation of the compounds of the elements being determined. This type of interference affects $\varepsilon$ and $\beta$ and therefore has exactly the same effect on all atomic spectrometric methods, assuming the same type of atomizer is used for each method. Chemical interferences in flame can be removed with releasing agents (eg; $La^{+3}$ releases $Ca^{+2}$ interference from $PO_4^{-3}$), or by using hotter flames, or both.

Physical interferences influence the aspiration efficiency ($\varepsilon$) and solution transport rate (F) and therefore have exactly the same effect on all flame methods. However, this is not an important interference when a graphite filament atomizer is employed.

There are two other types of interferences which occur often in atomic fluorescence spectrometry: scattering interferences and quenching interferences. The scattering interference is due to the scattering of source radiation by particles in the atom cell. In atomic fluorescence with a line excitation source, the scattering signal can be measured by using a nearby fluorescence line of similar intensity to the resonance line. If a continuum excitation source is used, the scattering interferences can be corrected by simply scanning the wavelength region containing the spectral line.

Quenching interferences occur when excited atoms are deactived by collisions with interferent species in the atom cell. The quenching efficiency of atoms in the graphite-filament atomizer is smaller than with the flame atomizer, because the graphite-filament atomizer is surrounded with inert gases (eg: Ar, He, etc.), whereas the flame atomizer has gaseous environments containing quenchers (eg: $N_2$, CO, $CO_2$, etc.). Therefore, more intense fluorescence will be obtained from a graphite-filament atomizer than from a flame atomizer. Assuming equal concentrations and source characteristics are utilized, the quenching ratio is defined as

$$Q = \frac{Y'_g}{Y'_f} \tag{II-9}$$

where

$Y'_g$ = the quantum efficiency of fluorescence of the analyte in the graphite-filament atomizer,

$Y'_f$ = the quantum efficiency of fluorescence of the analyte in flame cell.

The ratio Q has been expressed as (66)

$$Q = \frac{K_F + \Sigma_i (K_{Qi} N_{Qi})_g}{K_F + \Sigma_i (K_{Qi} N_{Qi})_f} \tag{II-10}$$

where

$K_F$ = the first order rate constant for radiational deactivation of the resonance level ($s^{-1}$)

$K_{Q_i}$ = the second order quenching rate constant for collision of element M with a quencher $Q_i$ ($cm^3\ s^{-1}$),

$n_{Q_i}$ = the concentration of the quencher ($cm^3$).

The summation is taken over all quenchers and subscripts g and f denote the use of graphite-filament atomizer and flame atomizer. Because the concentration of quenchers with graphite-filament atomizers surrounded by inert gas is very small,

$$K_F >> \Sigma_i\ (K_{Q_i}\ n_{Q_i})_g\ . \qquad \text{II-11}$$

Substituting equation II-11 into equation II-10, we have

$$Q = \frac{K_F}{K_F + \Sigma_i\ K_{Q_i}\ n_{Q_i}}\ . \qquad \text{II-12}$$

In most cases of analytical flames, $K_F$ = 1/10 of $\Sigma_i\ K_{Q_i}\ n_{Q_i}$, therefore equation II-12 will become

$$Q = \frac{K_F}{\Sigma_i\ K_{Q_i}\ n_{Q_i}}\ . \qquad \text{II-13}$$

According to equation II-13 the Q factor is about 10, which leads to the conclusion that the analyte atoms emit fluorescence approximately 10 times more intensely in the inert atmosphere of a graphite-filament atomizer than that of a flame cell.

## Time Constant Consideration of the Measurement System

For the transient peak height measurements, which are performed mostly in the measurement of fluorescence intensity of analyte with a graphite-filament atomizer; L'vov (66) has experimentally shown that if the time constant of the measurement circuit is approximately equal to the average residency time of the analyte in the cell for a transient signal, the highest value of signal-to-noise ratio will be obtained. The average residency time varies with various atomization temperatures' heating rates, coverage of the filament with analyte. If the atomization temperature is lower than the optimum value, then the peaks become broader and smaller as more time is required to evaporate the sample. However, increasing the atomization temperature beyond the optimum value does not result in sharper peaks. Instead, the peak retains the same width and merely loses height if the measurement system does not respond fast enough to the transient signal. Therefore, in order to obtain the best signal-to-noise ratio, the optimum time constant of the measurement system at the optimum atomization temperature should be used for the measurements of each element.

## Sheathing Gas Consideration

To prevent oxidation of sample and graphite, the graphite-filament is surrounded by an inert gas. Various gases can be used and the proper choice will often depend on whether absorption or fluorescence spectrometry is utilized. The influence of various inert gases on the fluorescence peak height measurements depends principally on the diffusion coefficient (D) of each gas. According to the kinetic theory of gases, the diffusion coefficient D is roughly inversely proportional to the square root of the mass (M) and to the square of the diameter of the surrounding molecules (d)

$$D \propto \frac{1}{d^2 M^{\frac{1}{2}}} \qquad \text{II-14}$$

It was reported that the residence time of the analyte free atoms in the sample cell of the carbon rod atomizer is inversely proportional to the diffusion coefficient (67). If the fluorescence peak height is measured for analyte atoms produced with a graphite-filament atomizer surrounded by an inert gas (as Ar) with a smaller diffusion coefficient, a much sharper fluorescence peak is obtained than when the atomizer is surrounded by an inert surrounding gas (He) with a larger diffusion coefficient.

## Noise Considerations

In any spectrochemical method of analysis a number of noise sources are present. When the noises from two or more independent sources are combined, the quadratic content of the resultant noise signal, $\Delta\bar{E}_T$, is the sum of the individual quadratic components (assuming the noises are independent).

$$\Delta\bar{E}_T = (\Delta\bar{E}_1^2\ \Delta f + \Delta\bar{E}_2^2\ \Delta f + \Delta\bar{E}_3^2\ \Delta f + \ldots)^{\frac{1}{2}} \qquad \text{II-15}$$

where $\Delta f$ is the frequency response bandwidth of the amplifier-readout system.

In flame atomic fluorescence spectrometry, the major sources of noise are flame flicker noise and phototube shot noise. When using higher temperature, fuel-rich flames, the flame flicker noise may be several orders of magnitude larger than shot noise. With the graphite-filament atomizer, the total noise is mainly amplifier noise, shot noise due to fluorescence flux, black body radiation and shot noise due to the graphite-filament. When using a properly baffled graphite-filament atomizer to reduce the shot noise from black body radiation of the graphite-filament atomizer, the noise level can be reduced to a minimum, thus providing another advantage of the graphite-filament atomizer as an atomization device over a flame atomizer.

## Limit of Detection

Assuming the readout noise is white (random noise) and readout drift is absent, the readout signal to noise ratio $(S/N)_{C_m}$, at the limiting detectable concentration $C_m$, for any instrumental technique, for any confidence level, and for any number of sample background pair observations p, can be derived as (68)

$$(S/N)_{C_m} = \frac{t\ 2^{\frac{1}{2}}}{p^{\frac{1}{2}}} \qquad \text{II-16}$$

where

t = student's "t", which depends upon the desired confidence level, (eg: 99.5%) and upon the number of degrees of freedom associated with the measurements ie., 2p-2,

p = the number of pairs of sample-background measurements.

If t is chosen to be 3, which results in a confidence level of 99.5%, and p is chosen to be 5, then the above equation would result in

$$(S/N)_{C_m} = \frac{3\ 2^{\frac{1}{2}}}{5^{\frac{1}{2}}} \approx 2 \qquad \text{II-17}$$

Thus the limiting detectable concentration is the concentration which produces a signal which is equivalent to two times the root mean square noise. If the only major random errors are due to electrical and optical noises, then the root mean square noise is defined as approximately the peak-to-peak noise divided by 5.

# CHAPTER III

# EXPERIMENTAL

## Reagents

A 500 ppm Conostan D-20 metallo-organic standard (Conostan Division, Continental Oil Company, P.O. Box 1267 Ponco City Oklahoma 74601 (405) 762-3456), containing Ag, Al, B, Ba, Be, Cd, Cr, Cu, Fe, Mg, Mn, Mo, Na, Ni, Pb, Si, Sn, Ti, V and Zn was used as the stock solution. Conostan metallo-organic standard is prepared by mixing metallo-organic sulfonate with oil base. Conostan metallo-organic standard (500 ppm) has excellent storage ability, and has shown no analytical evidence of change over a year's storage. When the stock standard is diluted to low concentration levels, some metals show a change in 3-4 months. This standard is not volatile (0.07% in one hour at 250$^{\circ}$F and 760 mm Hg pressure), and soluble in ketones, paraffins, and aromatic hydrocarbons. The analytical standard solutions were made by successive dilution of the Concostan metallo-organic standard (500 ppm) with isooctane (2,2,4-trimethylpentane) except for the Co and Tl standard solutions, which were prepared by successive dilution of aqueous Co and Tl stock standard solutions with demineralized water. The Co and Tl stock solutions were made by dissolving their respective analytical grade reagents with demineralized water.

## Experimental System

A schematic diagram of the experimental components of the instrument used in this work is shown in Figure 5. The components of this system

Fig. 5 - Schematic diagram of an atomic fluorescence spectrometer with an EIMAC continuum source and a graphite-filament atomizer.

B - illuminator power supply for EIMAC xenon arc lamp

E - EIMAC xenon arc lamp

$L_1$, $L_2$, $L_3$ - lenses

$S_1$, $S_2$ - apertures

C - chopper

F - graphite-filament atomizer

M - monochromator

P - photomultiplier tube

V - high voltage power supply

A - preamplier

L - lock-in amplifier

R - recorder readout

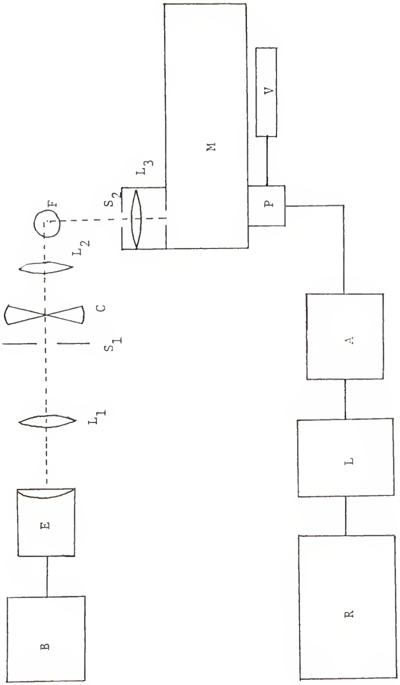
B
E
L$_1$
S$_1$
C
L$_2$
F
S$_2$
L$_3$
M
V
P
A
L
R

are discussed in detail below:

## Source of Excitation

A 150W EIMAC xenon arc lamp (Model VIX-150 UV, Varian Eimac Division, San Carlos, CA 94070) was used as the spectral excitation source. The EIMAC xenon arc lamp is a high pressure, short arc xenon lamp with aluminum parabolic reflector which enables virtually all the radiation from the point source to reach the atomizer. The lamp was operated at the manufacturer's recommended setting (12V, 12.5A) using an EIMAC power supply. The spectral output of the lamp drops off below 250 nm; however, some fraction of the output is still available down to about 210 nm allowing excitation of almost every element of interest (see Figure 6). In addition, this lamp has a long lifetime (about 1000 hr), is convenient to operate, and is very stable after a few minutes of warm-up time (Figure 7).

## Optical System

$L_1$, $L_2$, and $L_3$ in Figure 5 are all optical grade biconvex quartz lenses with a diameter of 2 in and a focal length of 2.0 in ($L_1$ and $L_2$) and 2.5 in ($L_3$)(Esco Products, Oak Ridge, NJ) and were used throughout for focusing. The lenses were mounted on a steel plate with the aid of magnetic mounts (Model M 8-1, Enco Manufacturing Co., Chicago, Ill.) and were aligned both vertically and horizontally with a He-Ne laser (Model ML 6805, Metrologic, Bellmaur, NJ). For atomic fluorescence measurements, the source radiation was focused to a 4 mm diameter image whose center was 3 mm above the graphite-filament atomizer by $L_1$ and $L_2$. The aperture $S_1$ in Figure 5 has a hole of diameter 1.0 cm in order to reduce the intensity of the unfocused light and minimize unfocused light entering the

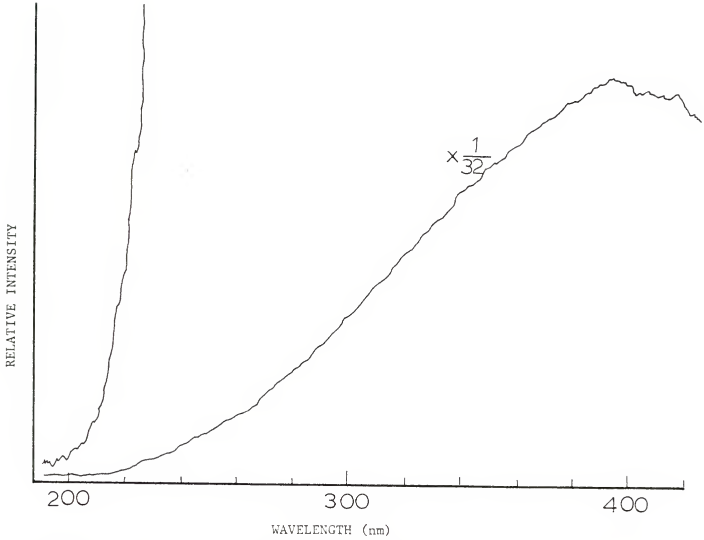

Figure 6. Spectral output of the EIMAC xenon arc continuum lamp used in this study. The lower curve has been scaled down by a factor of 32 compared to the upper curve.

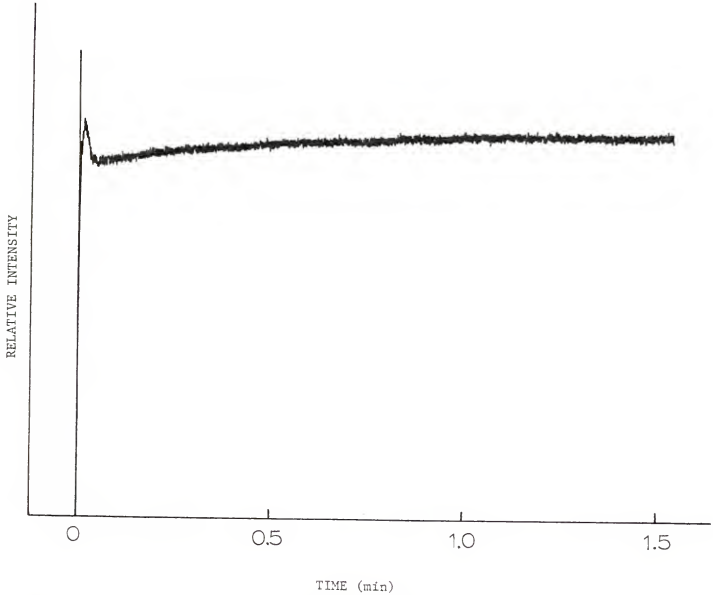

Figure 7. Time-stability of the EIMAC xenon arc continuum lamp used in this study.

monochromator. The aperture $S_2$ was adjusted so that the collected fluorescence would just fill the solid angle of the monochromator. All measurements were performed with a 0.35m f/6.8 Czernz-Turner monochromator (Model EU-700/E, Heath Co., Benton Harbor, Mich.).

## Electronic Measurement System

The electronic equipment used in these studies include a photomultiplier (PM) tube and its power supply, a lock-in amplifier, a preamplifier, a voltage divider and a recorder. The PM tube is an RCA IP 28 photomultiplier powered at 680 V by a high voltage power supply (Model EU-42A, Heath Co. ). The frequency of the lock-in amplifier (Model 391, Ithaco, Inc.,N.Y.) was tuned to 253 Hz. Source modulation was performed with a mechanical chopper (Model 382, Ithaco, Inc. ). The current from the PM tube was initially amplified by a variable gain preamplifier (Model 164, Ithaco, Inc. ), and then amplified by a lock-in amplifier. The output of the lock-in amplifier was reduced by a homemade voltage divider (10 mV full scale) and recorded on a fast response (0.5 s full-scale response), 10 mV full scale, potentiometric recorder (Model 212, Linear Instrumental Corp., Costa Mesa, CA 92626).

## Syringes

A hypodermic syringe (7101-N-CH, Hamilton Co., Whitter, CA) was used to dispense 0.5 μl of Conostan metallo-organic standard onto the graphite-filament cavity. A hypodermic syringe (Model 75, Hamilton Co. Whitter, CA) was used to dispense 1.0 μl of aqueous standard solutions onto the graphite-filament cavity.

## Atomizer

The graphite-filament atomizer, described by Molnar, Reeves and Winefordner (40) was used in these studies (see Figure 8). Power is supplied to the graphite-filament by a 300 A, 20 V DC supply (Model SCR-10-250, SCR Power Supply, Electronic Measurements, Inc., Oceanport, NJ) with the current time sequence controlled from a preset program in an adjustable timing circuit (40). The atomizer was used in conjunction with a flow of argon (6.3 l $min^{-1}$) and hydrogen (0.8 l $min^{-1}$) surrounding the graphite-filament to maintain the desired atmosphere around and above the filament.

### Measurement Procedures

The impurity on or in the graphite-filament was removed by preheating the filament a few times with a current of about 5 A greater than that necessary to atomize the elements. The graphite-filament was coated with a thin layer of pyrolytic carbon before any measurement by flowing methane (4.9 l $min^{-1}$), argon (5.2 l $min^{-1}$), and $H_2$ (1.3 l $min^{-1}$) over it at the current of 115 A (about 1750°C) for 7 s first, and then without interrupting, 150 A (about 2200°C) for 7 s. The procedure was similar to the one used by Clyburn, Knator, and Veillon (69). The aqueous standards were dispensed onto the cavity and dried using a current of 13 A (about 80°C) for 20 s.

The Conostan metallo-organic standards, SOAP standards and oil samples were dried at 20 A (about 200°C) for 10 s. and ashed at 43 A (about 400°C) for 20 s. The atomization currents varied with individual elements and were between 100 A to 140 A for 2.7 s. The experimental conditions for atomization are shown in Table 3.

### Rotameters Calibration

The rotameters were calibrated with a wet test method (Precision

Figure 8 - Schematic diagram of graphite-filament atomizer

a - bakelite block

b - copper cooling blocks

c - water inlet/outlet

d - terminal

e - clamping plates

f - graphite-filament

g - $H_2$/Ar(or/$CH_4$) gas inlet

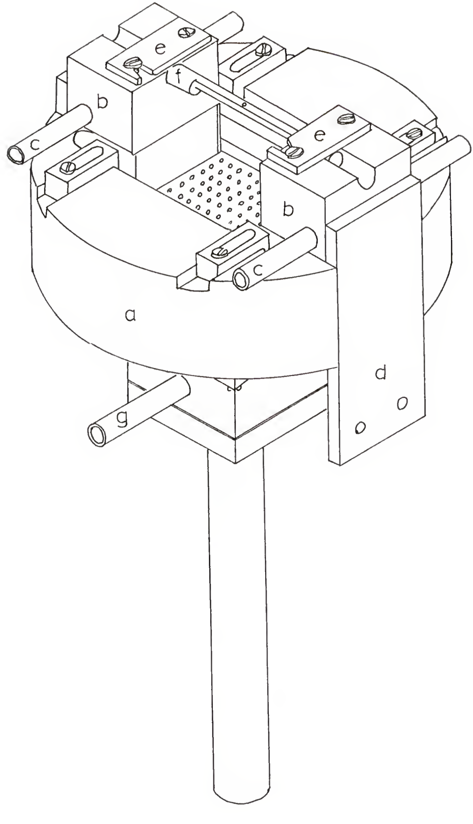
e
e
f
b
b
c
c
a
d
g

## TABLE 3

## EXPERIMENTAL CONDITIONS FOR ATOMIC FLUORESCENCE SPECTROMETER WITH EIMAC XENON ARC LAMP AND GRAPHITE-FILAMENT ATOMIZER

| Element | Wavelength[a] (nm) | Sample Size (μl) | Atomization[b] Temperature (°C) |
|---|---|---|---|
| Ag | 328.1 | 0.5 | 1500 °C |
| Cd | 228.2 | 0.5 | 1400 °C |
| Co | 240.7 | 1.0 | 1800 °C |
| Cr | 357.9 | 0.5 | 2000 °C |
| Cu | 320.7 | 0.5 | 1800 °C |
| Fe | 248.3 | 0.5 | 1800 °C |
| Mg | 285.2 | 1.0 | 2000 °C |
| Mn | 279.0 | 0.5 | 1700 °C |
| Ni | 232.0 | 0.5 | 1950 °C |
| Pb | 283.3 | 0.5 | 1500 °C |
| Sn | 317.5 | 0.5 | 1800 °C |
| Tl[c] | 377.6 | 1.0 | 1600 °C |
| Zn | 213.9 | 0.5 | 1800 °C |

[a] Monochromator slit width is 0.5 mm for all measurements

[b] Atomization time is 2.7 s for all elements

[c] Means aqueous standards

Scientific Co. ) for various gas flow rates of argon, hydrogen and methane, These calibration curves are shown in Figures 9-11.

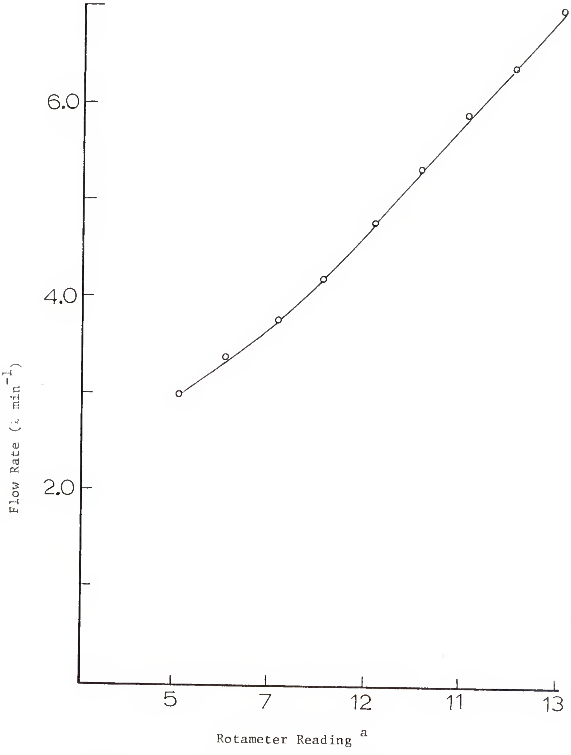

Fig. 9. Argon flow rate versus rotameter reading at 85 lb. pressure.

a. Reading at the center of silver ball.

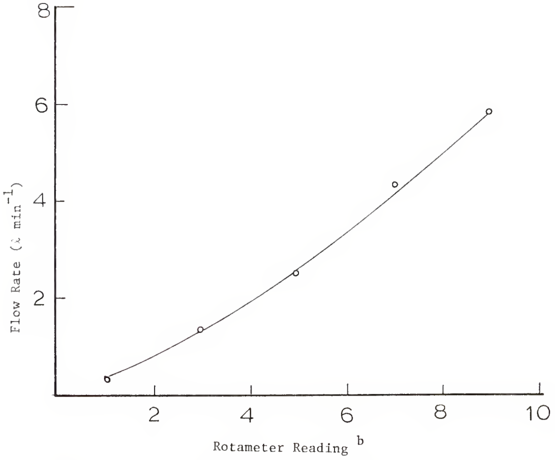

Fig. 10. Hydrogen flow rate versus rotameter reading at 8 lb. pressure.

b. Reading at the center of the black ball.

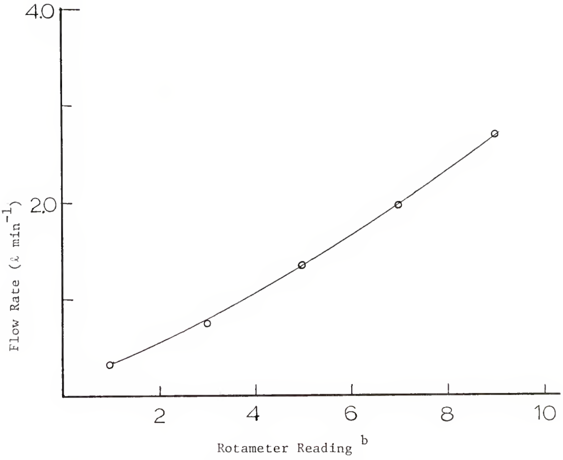

Fig. 11. Methane flow rate versus rotameter reading at 10 lb. pressure.

b. Reading at the center of the black ball.

# CHAPTER IV

# RESULTS AND DISCUSSION

## Formation of Pyrolytic Carbon on the Graphite-Filament

The reasons for coating a thin-layer of pyrolytic carbon on the graphite-filament were (i) to minimize scatter from hot carbon particles during the atomization cycle; (ii) to reduce the soaking of solutions into the filament body; (iii) to produce a surface with low gas permeability and which would heat uniformly; and (iv) to produce a surface resistant to air oxidation and with a long lifetime. In the present study, item (i) was of special importance because of the use of atomic fluorescence as the measurement technique. No appreciable scatter was observed when operating the pyrolytic graphite-filament at 150 A for 2.7 s for as many as 40 times or when operating the filament at 100-120 A for 2.7 s for as many as 120 times. After such periods of operation, appreciable scatter arose, and it was then necessary to remove the deteriorated pyrolytic surface and to re-pyrolyze the graphite-filament as discussed in the Experimental Section. Filaments prepared in this manner had an indefinite lifetime.

## Effect of Ar and $H_2$ Flow Rates Upon Atomic Fluorescence Signals

The use of a $H_2$- Ar entrained air flame rather than a purely inert gas shield has been previously discussed by Matoušek et al.(36,37) and by Molnar et al.(39). Reeves et al.(70-71) measured the spatial distribution of atomic absorption and atomic fluorescence signals above the graphite-filament when surrounded by pure argon or by an Ar/$H_2$ entrained air flame. The Ar/$H_2$ entrained air flame resulted in enhanced signals for several elements, the reason being most likely due to a lower oxygen concentration than when only Ar was used as the shield gas.

Ar was used in all studies as the inert gas. The reasons for this choice over He and $N_2$ were (i) lower cost than He; (ii) smallest diffusion coefficient; and (iii) small heat transfer coefficient (68); (iv) negligible quenching efficiency (other inert gases also have negligible quenching efficiency).

The influence of Ar flow rate upon the fluorescence signals can be summarized as: (i) the inert gas is a poor quenching species as well as poor compound former and so shields the analyte atoms from the better quenching, good compound formers (eg., oxygen) in the atmosphere; (ii) if the gas flow rate is too fast, turbulence occurs reducing the advantage listed in item (i) and diluting the analyte atom; and (iii) if the gas flow rate is too slow, then the gas shield is ineffective in shielding the analyte atoms from the atmosphere, and so the fluorescence signals decreased.

For all elements studied, plots of fluorescence signal vs Ar flow rate were bell-shaped with an optimum flow rate resulting in the best limits detection and relative standard deviations (see Figure 12).

For all elements studied, hydrogen gas increases the population of ground state atoms (via AA measurement); however, $H_2$ quenches radiationally excited atoms of various elements due to its relatively high quenching cross-section (compared to Ar) for deactivation of electronically-excited atoms. Therefore, the use of hydrogen as one component of the shielding gas will increase the fluorescence signals with respect to no hydrogen

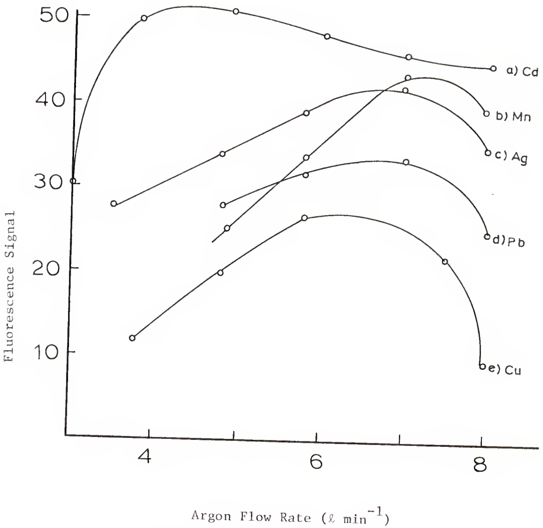

Fig. 12. Influence of argon flow rates on fluorescence signals of various elements.

flow only when the quenching effect of $H_2$ is less important than the atomization effect. As shown in Table 4, all the elements studied were atomized and excited in the presence of hydrogen as one component of shielding gas, except for Ag, Cd, Cu, Tl, and Zn which had lower detection limits without the flow of hydrogen. For those elements given in Figure 13, for which an increase in fluorescence signals occur with hydrogen present, the fluorescence signals increase with increasing hydrogen flow rate until a plateau is reached. For those elements, in which the fluorescence signals decrease with increase in hydrogen flow rate, a plateau at a constant low signal is reached (see Figure 13). At $H_2$ flow rates greater than 1.9 l $min^{-1}$, the relative standard deviation and detection limits deteriorate greatly due to the great turbulence resulting from mini-explosions above the filament.

## Influence of Methane Flow Rate Upon Atomic Fluorescence Signals

The pyrolysis treatment described in the Experimental Section could also be performed on a continuous basis by introducing a very low flow rate of methane gas (0.1 l $min^{-1}$) along with the Ar (6.2 l $min^{-1}$) and $H_2$ (0.8 l $min^{-1}$) gases while the atomic fluorescence measurements were being made. As can be seen from the plots in Figure 14, the presence of methane resulted in decreasing fluorescence signals for Ag, Cd, Cu, Mn, and Pb; in addition, the continuous flow of methane resulted in increasing light scatter and flicker noise.

Because the reduction in atomic absorption signals at a methane flow rate of 0.2 l $min^{-1}$ (35% for 0.5 ng Cd, 55.9% for 5 ng Cu, 81% for 1.0 ng of Mn, and 87% for 5 ng of Pb) paralleled the reduction in atomic fluorescence signals (35.7% for 0.5 ng Cd, 62.9% for 50 pg Cu, 77.8% for

TABLE 4

THE INFLUENCE OF HYDROGEN GAS UPON FLUORESCENCE AND ABSORPTION SIGNALS

| Element [a] | % of fluorescence signal [c,d,e], change at $H_2$ flow rate 0.8 l $min^{-1}$ with respect to 0 l $min^{-1}$ | % of absorbance change [c,d,e,f], at $H_2$ flow rate 0.8 l $min^{-1}$ with respect to 0 l $min^{-1}$ |
|---|---|---|
| Ag | -65.7% | +12.1% |
| Cd | -70.9% | +38.9% |
| Co [b] | +328% | +651% |
| Cr | +2250% | +2306% |
| Cu | -25.0% | +76.4% |
| Fe | +189% | +475% |
| Mg | +500% | +550% |
| Mn | +175% | +539% |
| Ni | +330% | +325% |
| Pb | +130% | +408% |
| Sn | +126% | —— |
| Tl [b] | -60% | —— |
| Zn | -53.8% | +846% |

TABLE 4 - continued

Footnotes

a. Conostan organo-metallic standard

b. Aqueous standard

c. The observation point of monochromator is 3 mm above graphite-filament

d. + means increasing signal, - means decreasing signal

e. Ar flow rate is 6.3 ℓ $\text{min}^{-1}$

f. Absorbances were measured by the same filament atomizer optical system with a DC electronic measurement equipment and hollow cathode lamps as line source.

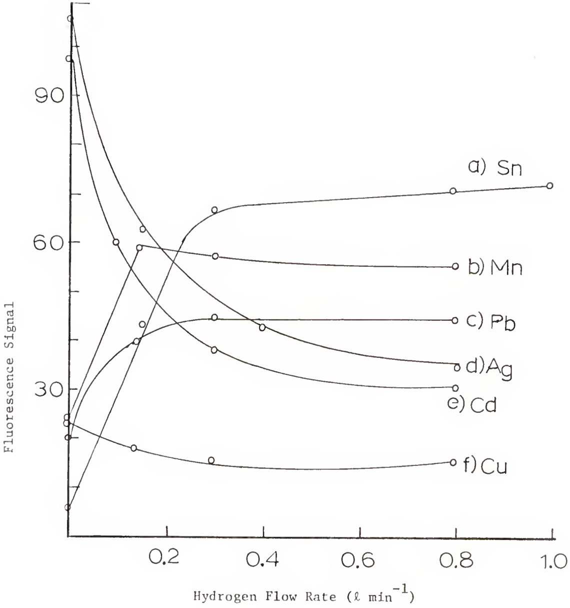

Fig. 13. Influence of hydrogen flow rates on fluorescence signals of various elements.

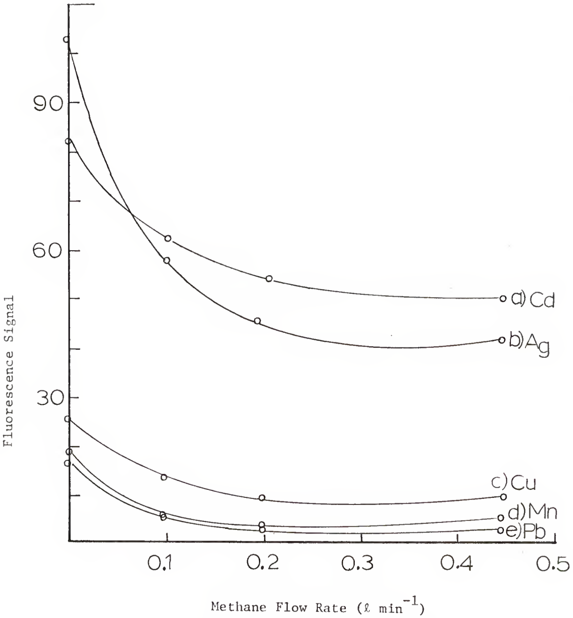

Fig. 14. Influence of methane flow rates on fluorescence signals of various elements.

50 pg Mn, and 84.2% for 5 ng Pb), the presence of methane (all other conditions are same as mentioned previously) during the spectral measurements produced a reduction in ground state atoms rather than an increase in quenching of the radiationally excited atoms. However, methane both reduced Ag ground state atoms (24% by AA measurement) and increased quenching of the radiationally excited atoms which resulted in decreasing fluorescence intensity (a 54% reduction). Therefore, continuous flow of methane during spectral measurements is not recommended except in those cases where a deterioration in detection limits and precision can be tolerated.

### The Influence of Height of Observation Upon Fluorescence Signals

The procedure for these measurements was similiar to that described by Reeves (70) and Patel (71). The variation of fluorescence signals of 8 elements (Ag, Cd, Co, Cr, Cu, Mg, Pb, and Sn) with the height of observation (ie., the distance between the graphite filament surface and the center of the light beam) with shielding gas being either Ar only or Ar/$H_2$ entrained air flame is shown in Figure 15 to Figure 22. The higher the observation point, the poorer are the detection limits and also the poorer are the relative standard deviations. The reasons are the increase in quenching opportunity of excited state atoms with quenchers ($N_2$, CO, and $CO_2$) in the atmosphere, the increase of the chances of compound formation, and the increase of the time for ground (and excited) state atoms to diffuse out of the observation point.

### The Influence of Time Constant of Lock-In Amplifier Upon Fluorescence Signals and Signal-to-Noise Ratios

L'vov (66) has shown theoretically and experimentally that the time

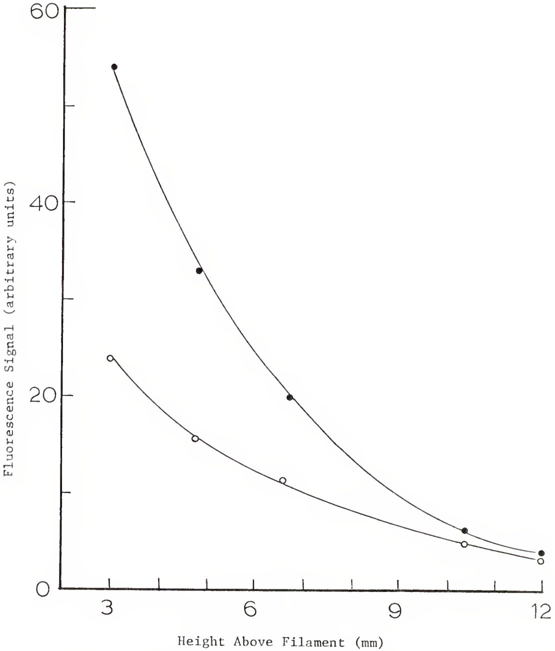

Fig. 15 Influence of height of observation upon silver fluorescence signals.

○—Ar/$H_2$ atmosphere (Ar : 5.8 ℓ $min^{-1}$; $H_2$ : 0.3 ℓ $min^{-1}$).

●—Ar atmosphere (5.8 ℓ $min^{-1}$).

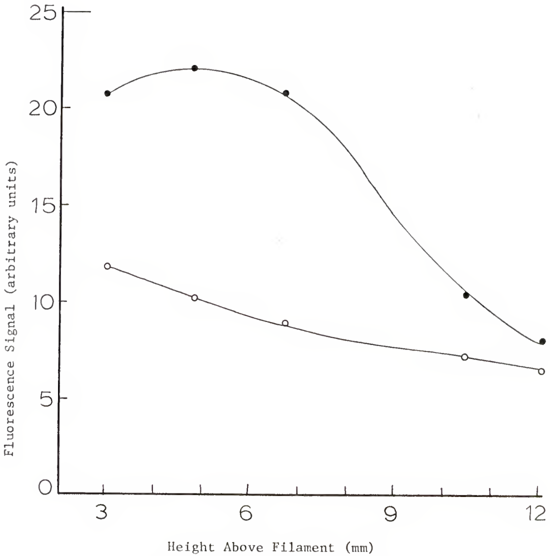

Fig. 16. Influence of height of observation upon cadmium fluorescence signals.

○— $Ar/H_2$ atmosphere (Ar : 5.8 ℓ $min^{-1}$; $H_2$ : 0.3 ℓ $min^{-1}$).

●— Ar atmosphere (5.8 ℓ $min^{-1}$).

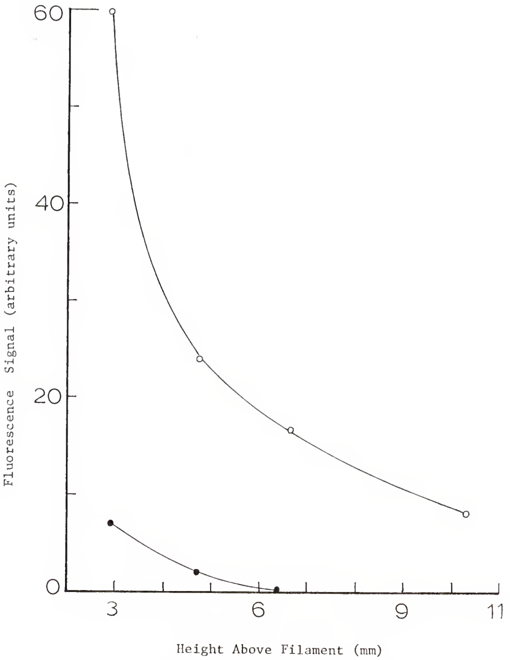

Fig. 17. Influence of height of observation upon chromium fluorescence signals.

○— Ar/$H_2$ atmosphere (Ar : 5.8 ℓ $min^{-1}$; $H_2$ : 0.3 ℓ $min^{-1}$).

●— Ar atmosphere (5.8 ℓ $min^{-1}$).

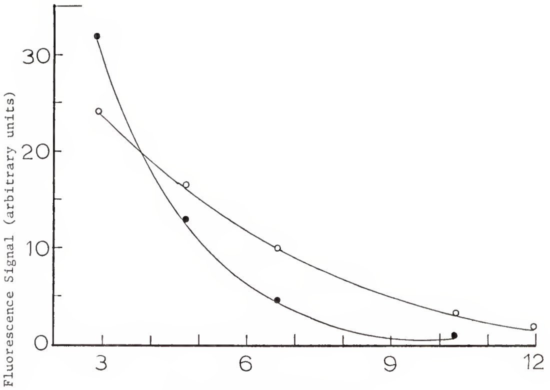

Fig. 18. Influence of height of observation upon copper fluorescence signals.

o— $Ar/H_2$ atmosphere (Ar : 5.8 ℓ $min^{-1}$; $H_2$ : 0.3 ℓ $min^{-1}$).

●— Ar atmosphere (5.8 ℓ $min^{-1}$).

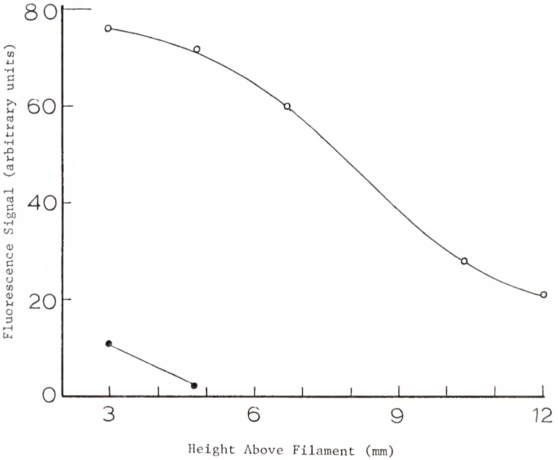

Fig. 19 Influence of height of observation upon iron fluorescence signals.

o—$Ar/H_2$ atmosphere (Ar : 5.8 ℓ $min^{-1}$; $H_2$ : 0.3 ℓ $min^{-1}$).

●—Ar atmosphere (5.8 ℓ $min^{-1}$).

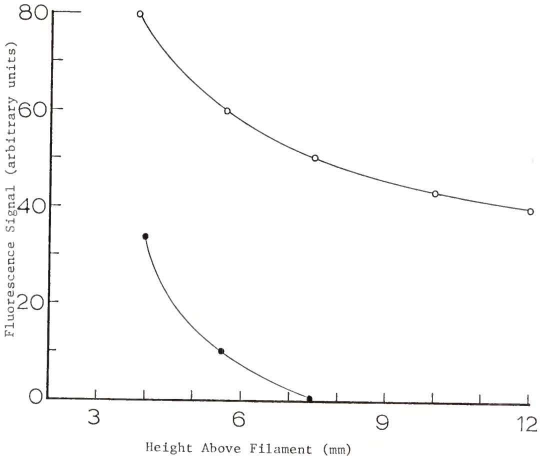

Fig. 20. Influence of height of observation upon magnesium fluorescence signals.

○— Ar/$H_2$ atmosphere (Ar : 5.8 ℓ $min^{-1}$; $H_2$ : 0.3 ℓ $min^{-1}$).

●— Ar atmosphere (5.8 ℓ $min^{-1}$).

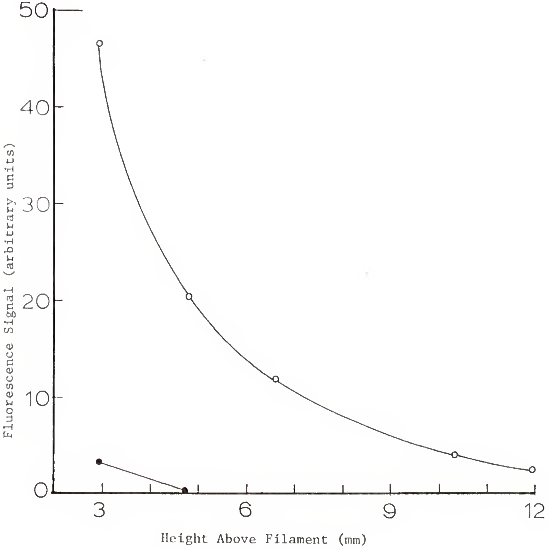

Fig. 21. Influence of height of observation upon tin fluorescence signals.

○ – Ar/$H_2$ atmosphere (Ar : 5.8 ℓ $min^{-1}$; $H_2$ : 0.3 ℓ $min^{-1}$).

● – Ar atmosphere (5.8 ℓ $min^{-1}$).

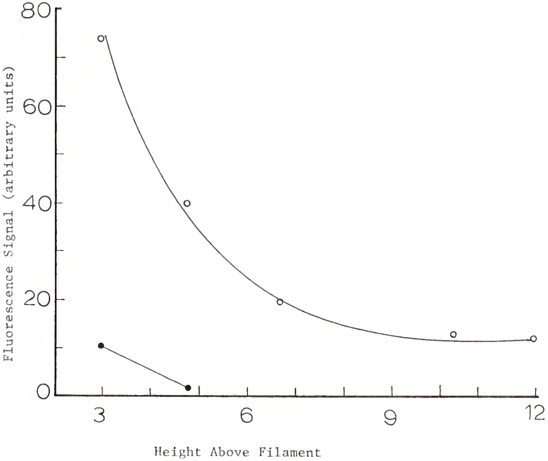

Fig. 22. Influence of height of observation upon lead fluorescence signals.

○ – Ar/$H_2$ atmosphere (Ar : 5.8 ℓ $min^{-1}$; $H_2$ : 0.3 ℓ $min^{-1}$).

● – Ar atmosphere (5.8 ℓ $min^{-1}$).

constant of the electronic measurement system should be approximately equal to the value of the average residency time of the analyte atoms within the observation region. Integration (66) of the time dependent signal also generally produces increased precision as compared to peak height measurements. West et al.(27) have shown that the measured signals decreased and became distorted as the time constant of the lock-in amplifier increased.

In the present study, the fluorescence signals and standard deviations of the fluorescence measurements were studied for each element as a function of time constant of the lock-in amplifier; time constants were optimized for the elements studied (other conditions are given in Table 3 ) to be: Ag - 125 ms; Cd - 40 ms; Co - 125 ms; Cr - 40 ms; Cu - 400 ms; Fe - 400 ms; Mg - 125 ms; Mn - 400 ms; Ni - 125 ms; Pb - 40 ms; Sn - 400 ms; Tl - 40 ms; and Zn - 40 ms.

## Analytical Figures of Merit

Atomic fluorescence analytical calibration curves (see Figure 23) were obtained by measuring the peak heights of the transient fluorescence signals for various amounts of analytes. Metallo-organic standards were used for all elements except Co and Tl for which aqueous standards were used (Experimental Section). The linear dynamic ranges (ratio of upper concentration or amount) at which linearity of the analytical calibration curve has deviated by 5% to the concentrational (or amount) limit of detection (concentration or amount) for the elements studied in this paper were: Ag - 1000; Cd - 200; Cu - 500; Co - 400; Cr - 220; Fe - 600; Mg - 1000; Mn - 670; Ni - 160; Pb - 85; Sn - 200; Tl - 800; and Zn - 200. These linear dynamic ranges are smaller than those normally obtained in

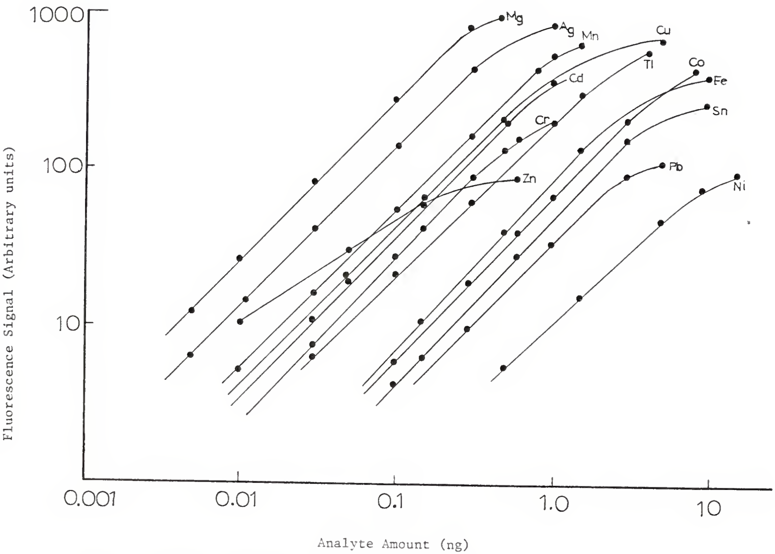

Fig. 23 Atomic fluorescence calibration curves for thirteen elements.

atomic fluorescence spectrometry with flame or non-flame atomizer and line sources. The detection limits (in μg/ml and in pg) for the above elements are listed in Table 5; for comparison purposes, detection limits obtained by several other atomic spectroscopic methods are listed. It is apparent that the detection limits (concentrational and absolute) obtained by the present versatile system involving an EIMAC continuum source are generally comparable (within an order of magnitude, in most cases) to those obtained by other atomic absorption, atomic fluorescence, and atomic emission spectrometric methods. The surprisingly low detection limits obtained in the present study are certainly a result of the relatively high, stable photon flux transferred from the EIMAC source to the atomic vapor and the efficient atomization of the analyte species by the graphite-filament atomizer.

## Precision

The precision of the measurements in this work is dependent upon the following factors: (i) the reproducibility of sampling small volumes (0.5 - 1.0 μl) and of placing the sample volumes in the filament cavity; (ii) the reproducibility of producing and maintaining atomic vapor concentration which depends upon the position of the cavity of the graphite-filament with respect to the intersection of the source atomizer and atomizer measurement system optical axis, ie., the filament should be adjusted close to the exciting light beam but should not reflect the exciting beam; if the filament is too far from the light beam, diffusion and molecular compound formation may cause losses (thus in the present study, a compromise was reached and the distance from the center of the focussed beam image to the top of the filament was made 3 mm; (iii) the

TABLE 5

LIMITS OF DETECTION MEASURED FOR SEVERAL ELEMENTS IN PRESENT WORK AND IN OTHER STUDIES

| Element-Wavelength (nm) | Limits of Detection,[a,b] µg/ml (pg) | | | | | | | |
|---|---|---|---|---|---|---|---|---|
| | Present Work (µg/ml) | Present Work (pg) | Flame AA(72) (µg/ml) | Flame AFL(62) (µg/ml) | Flame AFC (73) (µg/ml) | HGA-AA(59) (pg) | GF-AFL(27) (µg/ml) | GF-AFL(27) (pg) |
| Ag - 328.1 | 0.0006 | 0.3 | 0.001 | 0.0001 | 0.004 | 0.25 | 0.001 | 1. |
| Cd - 228.8 | 0.005 | 2.5 | 0.001 | 0.000001 | 0.01 | 0.1 | — | — |
| 326.1 | | | | | | | | |
| Co - 240.7 | 0.01 | 10. | 0.002 | 0.005 | 0.02 | 4. | — | — |
| Cu - 324.7 | 0.006 | 3. | 0.004 | 0.001 | — | 1. | — | — |
| 327.4 | | | | | | | | |
| Cr - 357.9 | 0.005 | 2.5 | 0.002 | 0.05 | 0.01 | 5. | — | — |
| Fe - 248.3 | 0.01 | 5. | 0.004 | 0.008 | — | 3. | — | — |
| 372.0 | | | | | | | | |
| Mg - 285.2 | 0.0002 | 0.2 | 0.003 | 0.001 | 0.0003 | — | 0.001 | 1. |
| Mn - 279.5 | 0.003 | 1.5 | 0.0008 | 0.006 | 0.004 | 1. | — | — |
| 403.1 | | | | | | | | |
| Ni - 232.0 | 0.1 | 50. | 0.005 | 0.003 | — | 10. | — | — |
| 352.4 | | | | | | | | |
| Pb - 217.0 | — | — | — | — | — | 6. | — | — |
| 283.3 | 0.07 | 35. | 0.01 | — | — | — | — | — |
| 405.7 | — | — | — | 0.01 | — | — | 0.01 | 10. |
| Sn - 235.4 | — | — | 0.05 | — | — | — | — | — |
| 286.3 | — | 1.5 | — | — | — | — | — | — |
| 303.4 | — | — | — | 0.05 | — | — | — | — |
| 317.5 | — | — | — | — | — | — | — | — |
| Tl - 276.8 | — | — | 0.02 | — | — | — | — | — |
| 377.6 | 0.004 | 4. | — | 0.008 | — | 14. | 0.05 | 50. |
| Zn - 213.9 | 0.002 | 1.0 | 0.001 | 0.00002 | 0.006 | 0.06 | 0.00002 | 0.02 |
| 334.5 | | | | | | | | |

TABLE 5 - continued

| Element-Wavelength (nm) | GF-AFL(50) (μg/ml) | GF-AFL(52) (μg/ml) | TF-AAL(49) (pg) | GF-AAL(39) (pg) | RF-AE(74) (μg/ml) |
|---|---|---|---|---|---|
| Ag - 328.1 | 0.002 | 0.0007 | 4. | 2. | — |
| Cd - 228.8 | — | 0.001 | 2. | — | — |
| 326.1 | | | | | 0.003 |
| Co - 240.7 | — | — | 300. | — | — |
| Cu - 324.7 | — | 0.002 | 10. | 12. | — |
| 327.4 | | | | | 0.0001 |
| Cr - 357.9 | — | 0.04 | 20. | 5. | 0.0003 |
| Fe - 248.3 | — | 0.02 | 100. | 5. | — |
| 372.0 | | | | | 0.0003 |
| Mg - 285.2 | — | 0.003 | 0.1 | 1. | 0.002 |
| Mn - 279.5 | — | 0.005 | 7. | — | — |
| 403.1 | | | | | 0.0006 |
| Ni - 232.0 | — | — | 200. | 60. | — |
| 352.4 | | | | | 0.0004 |
| Pb - 217.0 | — | — | 10. | — | — |
| 283.3 | 0.01 | 0.01 | | 75. | — |
| 405.7 | | | | | 0.002 |
| Sn - 235.4 | — | — | — | — | — |
| 286.3 | | 0.02 | 100. | — | — |
| 303.4 | 0.01 | | | | 0.03 |
| 317.5 | | | | | |
| Tl - 276.8 | — | — | — | — | — |
| 377.6 | 0.006 | — | 70. | — | — |
| Zn - 213.9 | — | 0.005 | 1. | — | — |
| 334.5 | | | | | 0.02 |

TABLE 5 - continued

Footnotes

a. Detection limits generally based upon concentration or amount giving a signal of 2X rms noise level. The detection limits are not necessarily the best but where possible are reported from a single source.

b. Abbreviations

Flame AAL = Atomic absorption flame spectrometry with line source

Flame AFL = Atomic fluorescence flame spectrometry with line source

Flame AFC = Atomic fluorescence flame spectrometry with continuum source

HGA-AAL = Perkin-Elmer graphite furnace atomic absorption spectrometry with line source

GF-AFL = Atomic fluorescence spectrometry with graphite-filament atomizer and line source

GT-AFL = Atomic fluorescence spectrometry with graphite tube furnace and line source (continuous sample introduction)

TF-AAL = Atomic absorption spectrometry with tantalum filament atomizer and line source

GF-AAL = Atomic absorption spectrometry with graphite-filament atomizer and line source

RF- AE = Radiofrequency inductively coupled plasma atomic emission spectrometry reproducibility of the size of the atomic vapor cloud excited which depends upon the image of the focussed light beam at the analyte atomic vapor; it should be small to maximize photon flux on a maximum number of analyte atoms (the incident beam was focussed to a 4 mm diameter range; no reflecting mirror was used to increase the source flux on the analyte atoms because of the difficulty of reflecting a good image of the source beam back onto the analyte atomic vapor); (iv) the reproducibility and magnitudes of the drying and ashing temperatures; they should be adjusted to avoid sample splattering; and (v) the reproducibility and magnitudes of the gas (Ar and $H_2$) flow rates; they should be adjusted as discussed before to maximize the fluorescence signals and signal-to-noise ratios.

The relative standard deviations of four measurements of each element were found to be: Ag(0.3 ppm; 0.5 $\mu$l) - 4.1%; Cd(0.8 ppm; 0.5 $\mu$l) - 4.3%; Co(1.0 ppm; 1.0 $\mu$l) - 3.4%; Cu(0.3 ppm; 0.5 $\mu$l) - 5.3%; Cr(0.3 ppm; 0.5 $\mu$l) - 6.2%; Fe(1.0 ppm; 0.5 $\mu$l) - 3.8%; Mg(0.05 ppm: 1.0 $\mu$l) - 7.0%; Ni(3.0 ppm; 0.5 $\mu$l) - 5.1%; Pb(1.0 ppm; 0.5 $\mu$l) - 5.5%; Sn(0.1 ppm; 0.5 $\mu$l) - 6.8%; Tl(0.3 ppm; 0.5 $\mu$l) - 6.1%; Zn(0.3 ppm; 0.5 $\mu$l) - 4.4%. These results are similar to those obtained with non-flame atomizers, previously.

# PART II - APPLICATIONS

## RAPID SEQUENTIAL ATOMIC FLUORESCENCE DETERMINATION OF SILVER AND COPPER

### Introduction

One specific feature of atomic fluorescence spectrometry (AFS) is its suitability to multielement analysis. Knapp and Winefordner (75) used a TV tube as a detector to perform AFS multielement analysis. Malmstadt and Cordos (76-80) used pulsed hollow cathode lamps (HCLs) and a programmed spectrometer which rapidly slewed between wavelengths for multielement analysis; in their work, a single photomultiplier tube was used and electrodeless discharge lamps (EDLs) were arranged around the flame atomizer to excite the elements. Johnson, Plankey, and Winefordner (81) determined trace wear metals in jet engine lubricating oils by atomic fluorescence flame spectrometry with an EIMAC continuum excitation source. Reeves, Molnar, and Winefordner (45) described a sequential atomization technique for the determination of silver and copper in jet engine oils via atomic absorption (AA) measurement and a multielement HCL by setting the monochromator wavelength at 327.4 nm and the spectra bandpass at 0.7 nm. Patel and Winefordner (46) simultaneously determined silver and copper in jet engine oils by AFS with a multielement EDL (containing Ag-Co-Cr-Cu-Fe-Mn-Ni-Pb-Sn) and a graphite-filament with only one atomization temperature (1527$^{\circ}$C).

In the present study, the sequential determination of silver and copper in jet engine oils with an EIMAC xenon arc lamp as a continuum excitation source and a graphite-filament as atomizer is described. The Ag and Cu fluorescence signals are temporally well separated. The analytical results are quite satisfactory compared with the mean value of the U.S. Air Force SOAP laboratory obtained by atomic absorption flame spectrometry.

## Experimental

The experimental system for this study has been described previously in PART I, CHAPTER III. The vertical distance between the center of the image of the incident beam and the graphite-filament was 3 mm. The monochromator was set at the wavelength of 327.5 nm with the spectral bandpass at 1.0 nm. SOAP (Spectrographic Oil Analysis Program) standard solutions containing 0 - 5.0 μg ml$^{-1}$ of silver 2-ethyl hexanoate and bis (1-phenyl-1, 3-butanedione) copper (II) were used to construct the analytical curves. A 0.5 μl of both standard solutions and samples were dispensed with a 1 μl syringe (7101 N-CH, Hamilton Co., Whitter, CA) into the 1 μl cavity of graphite-filament atomizer. The oil standards and oil samples are ashed at 400$^{o}$C for 20 s; the atomization temperature is set at 1000$^{o}$C (75 A) for 5 s (at this atomization condition, there is no observable Cu fluorescence signal) and then at 1640$^{o}$C (125 A) for 2.8 s, respectively. Both Ar (6.3 l min$^{-1}$) and $H_2$ (0.8 l min$^{-1}$) flowed above and around the graphite-filament atomizer as shielding gases. The time constant of the lock-in amplifier was set at 125 ms for all measurements in this work.

## Results and Discussion

Atomic fluorescence signals resulting from the sequential atomization of silver and copper for the two oil standards (0.4 ppm and 0.6 ppm) and an oil sample (73-4A) are shown in Figure 24. The temporal resolution between silver and copper fluorescence signals is quite satisfactory and resulted in precise AF peak height measurements. Because hydrogen quenches both silver and copper fluorescence signals, hydrogen is used as one component of the shielding gases to reduce the Ag and Cu fluorescence signals in order to eliminate the need of a dilution step due to the relatively high concentration of Ag and Cu in oil samples.

The analytical curves of Ag and Cu are shown in Figure 25. The upper absolute amount of concentration of Ag and Cu was not studied here; however, the concentrational limits of detection are 0.005 ppm for Ag and 0.04 ppm for Cu, respectively.

The analytical values of Ag and Cu in jet engine oils by this study in comparison with the mean values from the U.S. Air Force SOAP laboratory by flame atomic absorption method are shown in Table 6. There is good agreement between the SOAP values and our values; in addition, the standard deviations obtained in the present study are less than those resulting in the SOAP laboratory. The relative standard deviations for double measurements of nine oil samples are 2.6% - 8.8% for Ag, and 3.5% - 9.0% for Cu, which are similar to the results obtained previously (45,46).

Because each metallic element (or metallic oxide) has its own characteristic boiling point and because the EIMAC xenon arc lamp is a continuum excitation source, multielement analysis of several elements via a monochromatorless AFS system is definitely a possibility as long as the temperature of the graphite-filament is appropriately programmed.

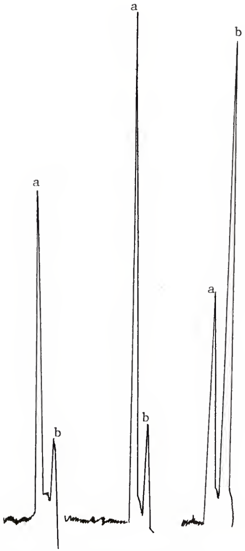

0.4 μg/ml Cu 0.6 mg/ml Cu

0.4 μg/ml Ag 0.6 mg/ml Ag    0.1 Sample (73-4A)

Fig. 24. Examples of temporal characteristic of atomic fluorescence signals resulting from sequential atomization of silver and copper.

a. silver
b. copper

(The scattering signal during ashing of the oil samples is not shown here).

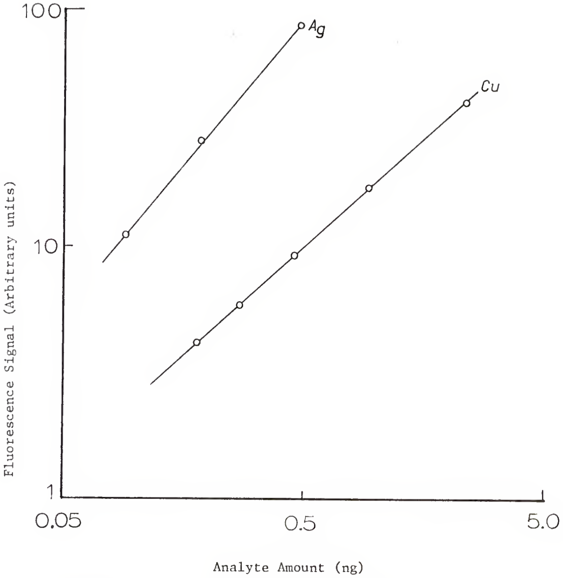

Fig. 25. Atomic fluorescence analytical calibration curves for sequential determination of silver and copper.

## TABLE 6

## COMPARISON OF SILVER AND COPPER DETERMINATIONS IN JET ENGINE OILS

| Sample | Ag Concentration ($\mu g\ ml^{-1}$) | | Cu Concentration ($\mu g\ ml^{-1}$) | |
|---|---|---|---|---|
| | (i) | (ii)(a) | (i) | (ii)(a) |
| 71-7A | 0.4±0.02 | 0.4±0.2 | 4.0±0.1 | 4.4±0.4 |
| 71-8A | 0.4±0.02 | 0.3±0.1 | 4.6±0.2 | 4.2±0.4 |
| 72-1A | 0.65±0.01 | 0.7±0.3 | 7.5±0.2 | 7.2±0.8 |
| 72-2A | 0.60±0.02 | 0.5±0.3 | 3.2±0.1 | 3.4±1.2 |
| 72-5A | 0.73±0.01 | 0.7±0.3 | 3.2±0.2 | 3.4±0.8 |
| 72-12A | 0.20±0.01 | 0.2±0.4 | 6.2±0.1 | 6.5±0.7 |
| 73-4A | 0.2±0.01 | 0.1±0.2 | 4.8±0.1 | 4.5±0.2 |
| 73-6A | 0.18±0.01 | 0.2±0.4 | 5.5±0.2 | 5.6±0.5 |
| 73-10A | 0.3±0.01 | | 1.6±0.05 | |

(i) Results of present work indicating the standard deviation represented as a ± value

(ii) U.S. Air Force S.O.A.P. Laboratory, flame atomic absorption method

(a) Standard deviation of results from the S.O.A.P. laboratories represented as a ± value

# REFERENCES

(1). R.W. Wood, Phil. Mag., 10, 513 (1905).

(2). E.L. Nichols and H.L. Howes, Phys. Rev., 23, 472 (1924).

(3). R.M. Badger, Z. Phys., 55, 56 (1929).

(4). C.Th.J. Alkemade, in Proceedings of Colloquium Spectroscopicum International, Spartan Books, Washington, D.C. 1963.

(5). J.D. Winefordner and T.J. Vickers, Anal. Chem., 36, 161 (1964).

(6). R.M. Dagnall, T.S. West, and P. Young, Talanta, 13, 803 (1966).

(7). R.F. Browner, B.M. Patel, T.H. Glenn, M.E. Rietta and J.D. Winefordner, Spectrosc. Lett., 5, 311 (1972).

(8). R.F. Browner and J.D. Winefordner, Spectrochim. Acta, 28B, 263 (1973).

(9). B.M. Patel, R.F. Browner, and J.D. Winefordner, Anal. Chem., 44, 2272 (1972).

(10). B.V. L'vov, J. Engng. Phys., 2 (2), 441 (1959).

(11). B.V. L'vov, J. Engng. Phys., 2 (11), 56 (1959).

(12). B.V. L'vov and G.G. Lebedev, Zh. Probl. Spectroskopii., 7, 264 (1967).

(13). B.V. L'vov, Spectrochim. Acta, 17, 761 (1961).

(14). B.V. L'vov, Spectrochim. Acta, 24B, 53 (1969).

(15). V.P. Borzov, B.V. L'vov, and G.V. Plyushch, J. Appl. Spectrosc., 11, 867 (1969).

(16). B.V. L'vov, Atomic Absorption Spectrochemical Analysis, Adam Hilger, London, 1970, page 193.

(17). H. Massmann, Spectrochim. Acta, 23B, 215 (1968).

(18). H. Massmann, Z. Analyst. Chem., 225, 203 (1967).

(19). R. Woodriff and G. Ramelow, "Graphite Tube Furnace for Atomic Absorption Spectrometry," paper presented at the National SAS Meeting, Chicago, 1966.

(20). R. Woodriff and G. Ramelow, Spectrochim. Acta, 23B, 665 (1968).

(21). R. Woodriff, R.W. Stone, and A.M. Held, Appl. Spectrosc., 22, 408 (1968).

(22). R. Woodriff and D. Shrafer, Anal. Chem., 43, 1918 (1971).

(23). J.F. Lech, D.D. Siemer, and R. Woodriff, Spectrochim. Acta, 28B, 435 (1973).

(24). D. Siemer, and R. Woodriff, Anal. Chem., 46, 597 (1974).

(25). R. Woodriff, Appl. Spectrosc., 28, 413 (1974).

(26). T.S. West and X.K. Williams, Anal. Chim. Acta, 45, 27 (1969).

(27). R.G. Anderson, I.S. Maines, and T.S. West, ibid., 51, 355 (1970).

(28). J.F. Alder, and T.S. West, ibid., 51, 365 (1970).

(29). J. Aggett and T.S. West, ibid., 55, 349 (1971).

(30). J. Agget and T.S. West, ibid., 57, 15 (1971).

(31). L. Ebdon, G.F. Kirkbright, and T.S. West, ibid., 58, 39 (1972).

(32). J.F. Alder and T.S. West, ibid., 58, 331 (1972).

(33). K.W. Jackson and T.S. West, ibid., 59, 187 (1972).

(34). G.L. Everett and T.S. West, ibid., 68, 387 (1974).

(35). M.J. Adams, G.F. Kirkbright, and T.S. West, Talanta, 21, 573 (1974).

(36). M.D. Amos, P.A. Bennett, K.G. Brodie, P.W.Y. Lung, and J.P. Matoušek, Anal. Chem., 43, 211 (1971).

(37). J.P. Matoušek and B.J. Steven, Clinic. Chem., 17, 363 (1971).

(38). K.G. Brodie and J.P. Matoušek, Anal. Chem., 43, 1557 (1971).

(39). C.J. Molnar, R.D. Reeves, and J.D. Winefordner, Appl. Spectrosc., 26, 607 (1972).

(40). R.D. Reeves, C.J. Molnar, M.T. Glenn, J.P. Ahlstrom, and J.D. Winefordner, Anal. Chem., 44, 2205 (1972).

(41). F.S. Chuang, B.M. Patel, R.D. Reeves, M.T. Glenn, and J.D. Winefordner, Can. J. Spectrosc., 18, 6 (1973).

(42). F.S. Chuang and J.D. Winefordner, Appl. Spectrosc., 28, 6 (1974).

(43). M.T. Glenn and J. Savory, S.A. Fein, R.D. Reeves, C.J. Molnar, and J.D. Winefordner, Anal. Chem., 45, 203 (1973).

(44). M. Glenn and J. Savory; L. Hart, T. Glenn, and J.D. Winefordner, Anal. Chim. Acta, 57,263 (1971).

(45). R.D. Reeves, C.J. Molnar, and J.D. Winefordner, Anal. Chem., 44, 1914 (1972).

(46). B.M. Patel and J.D. Winefordner, Anal. Chim. Acta, 64, 135 (1973).

(47). M.P. Bratzel, R.M. Dagnall, and J.D. Winefordner, Atomic Abs. Newsl., 7, 53 (1968).

(48). J.Y. Hwang, P.A. Ullucci, S.B. Smith Jr., and A.O. Malenfant, Anal. Chem., 43, 1319 (1971).

(49). J.Y. Hwang, C.J. Mokeler, and P.A. Ullucii, Anal. Chem., 44, 2018 (1972).

(50). C.J. Molnar and J.D. Winefordner, Anal. Chem., 46, 1418 (1974).

(51). T. Kantor, S.A. Clyburn, and C. Veillon, Anal. Chem., 46, 2205 (1974).

(52). S.A. Clyburn, B.R. Bartschmid, and C. Veillon, Anal. Chem., 46, 2201 (1974).

(53). G.F. Kirkbright, Analyst, 96, 609 (1971).

(54). J.D. Winefordner and T.J. Vickers, Anal. Chem., 44, 105R (1972).

(55). Ibid., 46, 192 R (1974).

(56). R. Woodriff, R.W. Stone, and A.M. Held, Appl. Spectrosc., 22, 408 (1968).

(57). J.Y. Hwang and G.P. Thomas, Amer. Lab., August, 55 (1974).

(58). E.H. Piepmeimer, Anal. Chem., 44, 2342 (1972).

(59). S. Slavin, W.B. Barnett, and H.L. Kahn, Atomic Abs. Newsl., 11, 37 (1972).

(60). N. Omenetto and J.D. Winefordner, Appl. Spectrosc., 26, 55, (1972).

(61). J.D. Winefordner, V. Svoboda, and L.T. Cline, CRC Crit. Rev., 1, 223 (1970).

(62). J.D. Winefordner and R.C. Elser, Anal. Chem., 43, 24A (1971).

(63). W.C. Campbell and J.M. Ottaway, Talanta, 21, 837 (1974).

(64). P.J.T. Zeeger, R. Smith, and J.D. Winefordner, Anal. Chem., 40 (13), 26A (1968).

(65). J.D. Winefordner, Pure Appl. Chem., 23, 35 (1971).

(66).. B.V. L'vov, Pure Appl. Chem., 23, 11 (1970).

(67). F.J.M.J. Maessen and R.D. Posma, Anal. Chem., 46, 1439 (1974).

(68). P.A. St. John, W.J. McCarty, and J.D. Winefordner, Anal. Chem., 39, 1495 (1967).

(69). S.A. Clyburn, T. Kantor, and C. Veillon, Anal. Chem., 46, 2213 (1974).

(70). R.D. Reeves, B.M. Patel, C.J. Molnar and J.D. Winefordner, Anal. Chem., 45, 246 (1973).

(71). B.M. Patel, R.D. Reeves, R.F. Browner, C.J. Molnar, and J.D. Winefordner, Appl. Spectrosc., 27, 171 (1973).

(72). G.D. Christian and F.J. Feldman, Appl. Spectrosc., 25, 660 (1971).

(73). D.J. Johnson, F.W. Plankey, and J.D. Winefordner, Anal. Chem., 46, 1898 (1974).

(74). P.W.J.M. Boumas and F.J. De Boer, Spectrochim. Acta, 27B, 391 (1972).

(75). D.C. Knapp and J.D. Winefordner, unpublished work, University of Florida, Gainesville, Fla. 32611, U.S.A.

(76). H.V. Malmstadt and E. Cordos, Amer. Lab., 4, 35 (1972).

(77). Ibid., Anal. Chem., 44, 2272 (1972).

(78). Ibid., Anal. Chem., 44, 2407 (1972).

(79). Ibid., Anal. Chem., 45, 425 (1973).

(80). Ibid., Anal. Chem., 45, 27 (1973).

(81). D.J. Johnson, F.W. Plankey, and J.D. Winefordner, Can. J. Spectrosc., 19, 151 (1974).

# BIOGRAPHICAL SKETCH

Feng-Shyong Chuang was born on April 10, 1945, in Taiwan, Republic of China. He received his degree of Bachelor of Science from National Chung Kung University, Taiwan, Republic of China in June, 1968. After a year's military service and another year's teaching at Nan-Chuang Junior High School, Mai-Li Hsian, Taiwan, Republic of China, he worked under the supervision of Dr. J.D. Winefordner toward the degree of Doctor of Philosophy at the Department of Chemistry, University of Florida. On November 10, 1972 he married Shirley Lin who received her Master of Business Administration degree in December, 1973.

I certify that I have read this study and that in my opinion it conforms to acceptable standards of scholarly presentation and is fully adequate, in scope and quality, as a dissertation for the degree of Doctor of Philosophy.

James D. Winefordner

James D. Winefordner
Professor of Chemistry

I certify that I have read this study and that in my opinion it conforms to acceptable standards of scholarly presentation and is fully adequate, in scope and quality, as a dissertation for the degree of Doctor of Philosophy.

Roger G. Bates

Roger G. Bates
Professor of Chemistry

I certify that I have read this study and that in my opinion it conforms to acceptable standards of scholarly presentation and is fully adequate, in scope and quality, as a dissertation for the degree of Doctor of Philosophy.

Gerhard M. Schmid

Gerhard M. Schmid
Associate Professor of Chemistry

I certify that I have read this study and that in my opinion it conforms to acceptable standards of scholarly presentation and is fully adequate, in scope and quality, as a dissertation for the degree of Doctor of Philosophy.

John E. Singley
Professor of Environmental Engineering

I certify that I have read this study and that in my opinion it conforms to acceptable standards of scholarly presentation and is fully adequate, in scope and quality, as a dissertation for the degree of Doctor of Philosophy.

Willis B. Person

Willis B. Person
Professor of Chemistry

This dissertation was submitted to the Graduate Faculty of the Department of Chemistry in the College of Arts and Sciences and to the Graduate Council, and was accepted as partial fulfillment of the requirements for the degree of Doctor of Philosophy.

June, 1975

Dean, Graduate School